

**Post-translational Protein Deimination Signatures in Sea Lamprey (*Petromyzon marinus*) Plasma and Plasma-Extracellular Vesicles**

Jonathan P. Rast<sup>a</sup>, Stefania D'Alessio<sup>b</sup>, Igor Kraev<sup>c</sup>, Sigrun Lange<sup>b\*</sup>

<sup>a</sup>*Emory University School of Medicine, Pathology & Laboratory Medicine, Atlanta GA 30322, USA; jprast@emory.edu*

<sup>b</sup>*Tissue Architecture and Regeneration Research Group, School of Life Sciences, University of Westminster, London W1W 6UW, UK; email: [S.Lange@westminster.ac.uk](mailto:S.Lange@westminster.ac.uk)*

<sup>c</sup>*Electron Microscopy Suite, Faculty of Science, Technology, Engineering and Mathematics, Open University, Milton Keynes, MK7 6AA, UK; igor.kraev@open.ac.uk*

\*Corresponding author: [S.Lange@westminster.ac.uk](mailto:S.Lange@westminster.ac.uk)

Accepted Manuscript Version

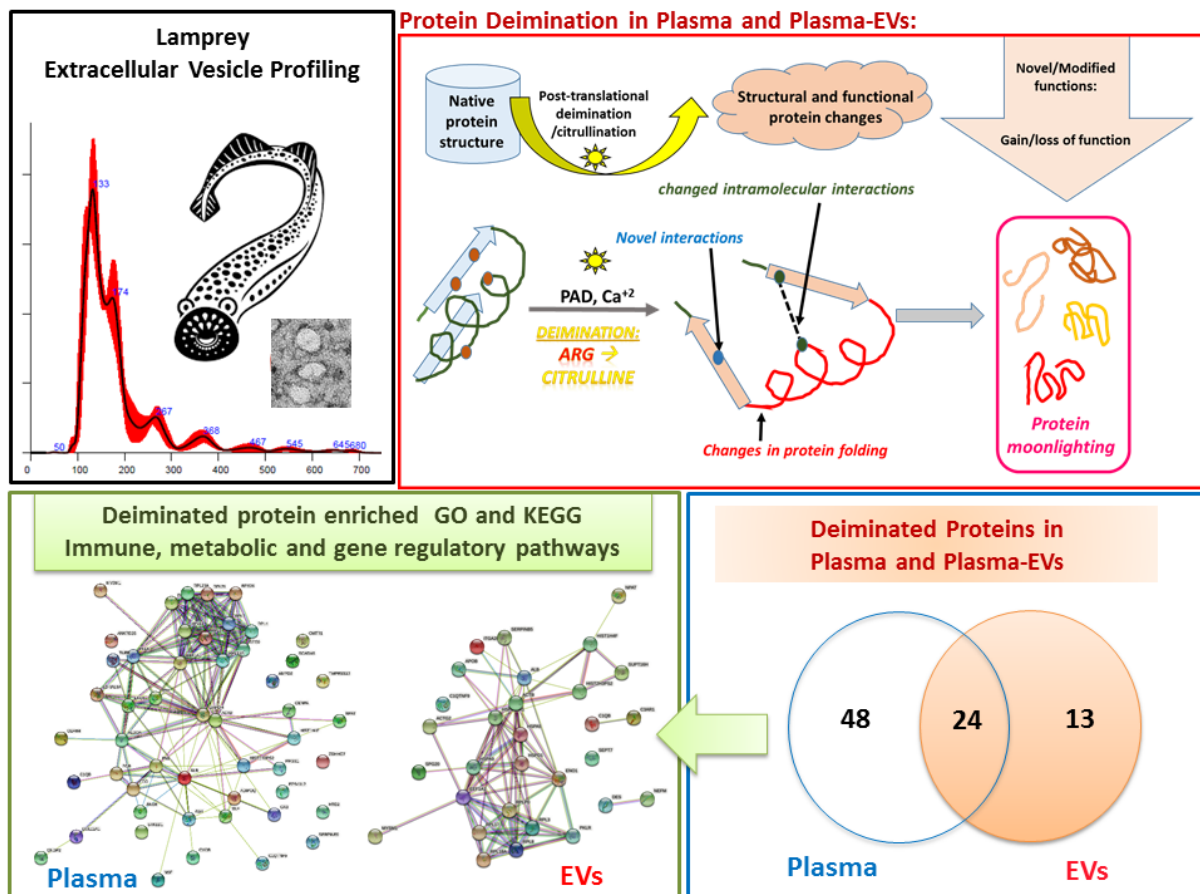
## Abstract

Lampreys are a jawless vertebrate species belonging to an ancient vertebrate lineage that diverged from a common ancestor with humans ~500 million years ago. The sea lamprey (*Petromyzon marinus*) has a filter feeding ammocoete larval stage that metamorphoses into a parasitic adult, feeding both on teleost and elasmobranch fish. Lampreys are a valuable comparative model species for vertebrate immunity and physiology due to their unique phylogenetic position, unusual adaptive immune system, and physiological adaptations such as tolerance to salinity changes and urea.

Peptidylarginine deiminases (PADs) are a phylogenetically conserved enzyme family which catalyses post-translational deimination/citrullination in target proteins, enabling proteins to gain new functions (moonlighting). The identification of deiminated protein targets in species across phylogeny may provide novel insights into post-translational regulation of physiological and pathophysiological processes. Extracellular vesicles (EVs) are membrane vesicles released from cells that carry cargos of small molecules and proteins for cellular communication, involved in both normal and pathological processes. The current study identified deimination signatures in proteins of both total plasma and plasma-EVs in sea lamprey and furthermore reports the first characterisation of plasma-EVs in lamprey. EVs were poly-dispersed in the size range of 40-500 nm, similar to what is observed in other taxa, positive for CD63 and Flotillin-1. Plasma-EV morphology was confirmed by transmission electron microscopy. Assessment of deimination/citrullination signatures in lamprey plasma and plasma-EVs, revealed 72 deimination target proteins involved in immunity, metabolism and gene regulation in whole plasma, and 37 target proteins in EVs, whereof 24 were shared targets. Furthermore, the presence of deiminated histone H3, indicative of gene-regulatory mechanisms and also a marker of neutrophil extracellular trap formation (NETosis), was confirmed in lamprey plasma. Functional protein network analysis revealed some differences in KEGG and GO pathways of deiminated proteins in whole plasma compared with plasma-EVs. For example, while common STRING network clusters in plasma and plasma-EVs included Peptide chain elongation, Viral mRNA translation, Glycolysis and gluconeogenesis, STRING network clusters specific for EVs only included: Cellular response to heat stress, Muscle protein and striated muscle thin filament, Nucleosome, Protein processing in endoplasmic reticulum, Nucleosome and histone deacetylase complex. STRING network clusters specific for plasma were: Adipokinetic hormone receptor activity, Fibrinogen alpha/beta chain family, peptidase S1A, Glutathione synthesis and recycling- arginine, Fructose 1,6-bisphosphate metabolic process, Carbon metabolism and lactate dehydrogenase activity, Post-translational protein phosphorylation, Regulation of insulin-like growth factor transport and clotting cascade. Overall, for the EV citrullinome, five STRING network clusters, 10 KEGG pathways, 15 molecular GO pathways and 29 Reactome pathways were identified, compared with nine STRING network clusters, six KEGG pathways, two Molecular GO pathways and one Reactome pathway specific for whole plasma; while further pathways were shared. The reported findings indicate that major pathways relevant for immunity and metabolism are targets of deimination in lamprey plasma and plasma-EVs, with some differences, and may help elucidating roles for the conserved PAD enzyme family in regulation of immune and metabolic function throughout phylogeny.

**Key words:** peptidylarginine deiminase (PAD); protein deimination/citrullination; extracellular vesicles (EVs); lamprey; immunity; metabolism; gene regulation.

## GRAPHIC ABSTRACT



## Introduction

Lampreys are representatives of the jawless vertebrates that today include about 40 species of lampreys and 80 species of hagfish. This ancient vertebrate lineage diverged from the lineage leading to humans ~500 million years ago (Kuraku and Kuratani, 2006). The sea lamprey (*Petromyzon marinus*) is native to the Northern Atlantic with a complex life cycle in which a filter-feeding, fresh water ammocoete larval form metamorphoses into a parasitic, marine adult form that feeds on both teleosts and elasmobranchs. In the course of this life cycle, sea lamprey are tolerant to a wide range of salinities and can tolerate high levels of urea, which allows them to parasitise sharks and other elasmobranchs (Wilkie et al., 2004). The lamprey genome has been sequenced (Smith et al., 2013, Smith et al. 2018) and been a key model in the study of vertebrate developmental evolution (e.g., Xu et al., 2016; York and McCauley, 2020), while much attention has also focussed on lamprey immunity (Pancer 2004, Boehm et al., 2018). The lamprey adaptive immune system differs strikingly from that of jawed vertebrates as lampreys and the hagfishes lack immunoglobulins but have three types of variable lymphocyte receptors (VLRs) (Alder et al., 2005; Guo et al., 2009; Hirano et al., 2013; Boehm et al., 2018). The complement system of lamprey also displays unique features, indicating that certain aspects have developed independently from jawed vertebrates (Dodds and Matsushita, 2007; Matsushita, 2018). Due to its phylogenetic position as a connection to a rich and early phase of vertebrate evolution, the lamprey is an important model species for assessing the conservation and divergence of vertebrate characteristics.

PADs are a phylogenetically conserved calcium-dependent family of enzymes with multifaceted roles in health and disease. PADs convert arginine into citrulline in an irreversible manner, leading to post-translational modification (deimination/citrullination) in numerous target proteins of cytoplasmic, nuclear and mitochondrial origin (Vossenaar, 2003; György et al., 2006; Magnadóttir et al., 2018a,b; Magnadóttir et al., 2019a; Criscitiello et al., 2020a; Alghamdi et al., 2019). Deimination causes structural protein changes which can affect protein function and consequently downstream protein-protein interactions. Deimination can contribute to neo-epitope generation, resulting in inflammatory responses, and also affect gene regulation via deimination of histones (Bicker and Thompson, 2013; Wang and Wang, 2013; Witalison et al., 2015; Lange et al., 2017; Mondal and Thompson, 2019). PADs are furthermore one key-driver of neutrophil extracellular trap formation (NETosis), a phylogenetically conserved anti-pathogenic mechanism (Brinkmann et al., 2004; Palić et al., 2007; Claushuis et al., 2018), which is partly attributed to deimination of histone H3 (Deng et al., 2020; Zuo et al., 2020). In mammals five PAD isozymes are known (PAD1, 2, 3, 4, 6), whereof PAD2 is considered the most phylogenetically conserved isozyme, while three PAD isozymes have been described in birds and reptiles, but only one PAD form (PAD2 like) is reported in teleost and cartilaginous fish (Vossenaar et al., 2003; Rebl et al., 2010; Magnadóttir 2018a, Magnadóttir et al., 2019a; Criscitiello et al., 2019; Criscitiello et al., 2020a,b). Furthermore, PAD homologues, also referred to as arginine deiminases (ADI) (Novák et al., 2016) are described from outside of animals, including in parasites (Gavinho et al., 2020; Kristmundsson et al., 2021), bacteria (Bielecka et al., 2014; Kosgodage et al., 2019) and fungi (El-Sayed et al., 2019). In lamprey, PAD2-like protein sequences have indeed been reported (XP\_032825558.1; XP\_032825490.1; XP\_032825520.1), but no studies relating to lamprey PAD activity have hitherto been published.

PADs and downstream protein deimination are related to numerous human pathological mechanisms, but have recently gained momentum in comparative animal models. This body of work has focussed on identifying putative roles for PADs and deimination in physiological and immunological pathways in taxa across the phylogenetic tree, including land and sea mammals, reptiles, birds, bony and cartilaginous fish, Myrostromata, Crustacea, Mollusca and Alveolata (Magnadóttir et al., 2018a, 2019a,b, 2020a,b,c; Phillips et al., 2020; Pamerter et al., 2019; Criscitiello et al., 2019,2020a,b; Bowden et al., 2020a,b,c; Kristmundsson et al., 2021). In these studies, PADs have indeed been identified to have roles in regulating pathways of mucosal, innate and adaptive immunity via post-translational deimination (Lange et al., 2019; Magnadóttir et al., 2018a and 2018b, 2019a; 2020a,b,c; Criscitiello et al., 2019, 2020a,b,c; Pamerter et al., 2019; Bowden et al., 2020a,b,c; Phillips et al., 2020; D'Alessio et al., 2021). Importantly, PADs have also been identified as significant players in host-pathogen interactions, including with viral (Muraro et al., 2018; Casanova et al., 2020), parasitic (Gavinho et al., 2020; Kristmundsson et al., 2021), and bacterial pathogens (Kosgodage et al., 2019; Bieleika et al., 2014). As post-translational changes contribute to protein moonlighting, which allows one protein to exhibit different functions within one polypeptide chain (Henderson and Martin, 2014; Jeffrey, 2018), deimination may be one such mechanism facilitating functional diversity of proteins. As experimentally based information on deimination as a regulator of protein function is still relatively limited, studies aimed at identifying deimination mediated regulation of homologous and conserved proteins in the phylogenetic tree could provide information on the diversification of immune and metabolic pathway function throughout evolution.

Extracellular vesicle (EV) biogenesis, and regulation of cellular EV release, has been shown to be partly controlled by PADs (Kholia et al., 2015). This function appears to be phylogenetically

conserved and has been identified in bacteria, parasites and mammals (Kholia et al., 2015; Gavinho et al., 2020; Kosgodage et al., 2017, 2018, 2019; Uysal-Onganer et al., 2020). EVs participate in cellular communication, are found in most body fluids and can readily be isolated from serum and plasma. EVs play physiological and pathological roles via transfer of cargo proteins and genetic material, in biological processes such as inflammatory responses, in infection and host-pathogen interactions (Inal et al., 2013; Colombo et al., 2014; Lange et al., 2017; Antwi-Baffour et al., 2019; Turchinovich et al., 2019; Vagner et al., 2019; Gavinho et al., 2020). As EVs carry information from their cells of origin, their cargo signatures, including deimination signatures, can act as usable biomarkers (Hessvik and Llorente, 2018; Ramirez et al., 2018; Magnadottir et al., 2020a). Recent EV research in aquatic species across phylogeny has included marine mammals such as pinnipeds and cetaceans (Magnadottir et al., 2020b,c), teleost fish (Iliev et al., 2018; Magnadottir et al., 2019; Lange et al., 2019; 2020a; Magnadottir et al., 2021), cartilaginous fish (Criscitiello et al., 2019), Merostomata (Bowden et al., 2020a), Crustacea (Yang et al., 2019; Bowden et al., 2020b) and Mollusca (Bowden et al., 2020c). Here we extend these ongoing studies in our laboratories on EV characterisation and protein deimination signatures, including in EV cargo as indication for roles in intracellular trafficking, in the Agnatha using sea lamprey as a model species.

The current study characterised plasma-EVs from sea lamprey and assessed post-translational deimination signatures in proteins from plasma and plasma-EVs. Our findings provide novel insights into post-translational regulation of pathways in lamprey immunity and metabolism and add to current understanding of putative roles for post-translational deimination in functional diversification of conserved immune, gene regulatory and metabolic proteins throughout phylogeny.

## **2. Materials and Methods**

### **2.1 Neighbour-joining Tree Construction for PAD2-like Protein from Lamprey**

For reconstruction of a phylogeny tree for lamprey PAD, previously reported PAD2-like protein sequences of lamprey (XP\_032825558.1, XP\_032825490.1, XP\_032825520.1) were compared with teleost fish (sea bass – *Dicentrarchus labrax* CBN80708.1; rainbow trout – *Oncorhynchus mykiss* PAD protein CAX45844.1 and PAD type-2-isoform X2 XP\_021425236.1), reptilian (*Alligator mississippiensis* PAD1 XP\_006259278.3, PAD2 XP\_019355592.1 and PAD3 XP\_014457295.1\_PAD3), amphibian (*Xenopus laevis* PAD2 homologue NP\_001080369.1) and human PAD isozymes (PAD1 NP\_037490.2; PAD2 NP\_031391.2; PAD3 NP\_057317.2; PAD4 NP\_036519.2 and PAD6 NP\_997304.3). Neighbour joining tree construction was performed following protein sequence alignment, using Clustal Omega, and homology of lamprey PAD amino acid sequences compared with teleost, amphibian, reptilian and human PAD isozyme sequences was determined by percent identity matrix, using Clustal Omega (<https://www.ebi.ac.uk/Tools/msa/clustalo/>).

### **2.2 Sampling of Sea Lamprey Plasma**

Blood was collected from seven Atlantic coast sea lamprey (*Petromyzon marinus*) ammocoete larvae for the isolation of blood plasma, which was diluted in 200 µl 0.66x PBS, 50 mM EDTA. The diluted plasma aliquots (approximately 250 µl per individual animal) were frozen at -80°C until used. All procedures were carried out according to protocols approved by the Emory University Institutional Animal Care and Use Committee (PROTO201700387, 2020).

### **2.3 Isolation of Extracellular Vesicles and Nanoparticle Tracking Analysis (NTA)**

Lamprey plasma EVs were prepared from the individual (n=7) blood plasma (thawed on ice), using sequential centrifugation and ultracentrifugation. Procedures were carried out according to previously standardised and described protocols (Kosgodage et al., 2018; Criscitiello et al., 2019; Pamerter et al., 2019; Phillips et al., 2020; Criscitiello et al., 2020b; Bowden et al., 2020a), also following recommendations of MISEV2018 (the minimal information for studies of extracellular vesicles 2018; Théry et al., 2018). For each individual plasma-EV preparation, 250 µl aliquots of the diluted plasma preparation was diluted 1:1 in DPBS, centrifuged for 30 min at 4,000 g at 4 °C, whereafter the supernatants were collected and ultra-centrifuged at 100,000 g at 4 °C for 1 h. This resulted in EV-enriched pellets, which were then resuspended each in 500 µl DPBS (“washing”) and thereafter ultra-centrifuged again for 1 h at 100,000 g, at 4 °C. The final resulting EV pellets were each resuspended in 100 µl of DPBS and analysed by nanosight particle tracking analysis (NTA), transmission electron microscopy (TEM), western blotting and proteomic analysis. For each of the procedures and assessments described below, EV pellets were kept frozen at -80 °C following isolation from plasma and used within one week. NTA analysis was used to quantify EVs and to assess EV size distribution profiles, using the NanoSight NS300 system (Malvern, U.K.), by diluting the EV samples 1/100 in DPBS (10 µl of EV preparation diluted in 990 µl of DPBS). For generation of the NTA size distribution curves, five 60 sec repetitive reads were performed per sample, using a 488 nm laser module and sCMOS camera, with particle numbers at 40 to 60 per frame. Camera settings were at level 9 for recording and detection threshold for post-analysis was set at 5. Replicate histograms were generated using the NanoSight software 3.0 (Malvern), representing mean and confidence intervals of the 5 recordings per sample.

#### **2.4 Transmission Electron Microscopy (TEM)**

Plasma EVs were further assessed for morphology using TEM. The procedure was similar as previously described (Criscitiello et al., 2020b; Phillips et al., 2020). EV pellets were thawed, resuspended in 100 mM sodium cacodylate buffer (pH 7.4) and one drop (~3-5 µl) placed onto a grid with a previously glow discharged carbon support film. Following partial drying of the EV suspension, the sample was fixed for 1 min at room temperature by placing the grid onto a drop of a fixative solution (2.5 % glutaraldehyde in 100 mM sodium cacodylate buffer (pH 7.0)). The grid was applied to the surface of three drops of distilled water for washing of the EV sample, removing excess water using a filter paper. The EVs were then stained for 1 min with 2 % aqueous Uranyl Acetate (Sigma-Aldrich), removing excess stain with a filter paper and air drying the grid. TEM Imaging of EVs was carried out using a JEOL JEM 1400 transmission electron microscope (JEOL, Tokyo, Japan), which was operated at 80 kV, using a magnification of 30,000x to 60,000x. Digital images were recorded using an AMT XR60 CCD camera (Deben, UK).

#### **2.5 Isolation of Deiminated Proteins in Lamprey Plasma and Plasma-EVs using F95 Enrichment**

Total deiminated proteins were isolated from lamprey plasma and plasma-EVs using the F95 pan-deimination antibody (MABN328, Merck) and the Catch and Release®v2.0 immunoprecipitation kit (Merck, U.K.), according to previously described methods (Criscitiello et al., 2020a; Bowden et al, 2020c). The F95-antibody is a pan-citrulline antibody which specifically detects proteins modified by citrullination/deimination (Nicholas and Whitaker, 2002). Pools of plasma from five individual animals (5 x 20 µl) and pools of the corresponding plasma-EVs from 5 individuals (5x20 µl) were used for F95-enrichment, which was performed at 4 °C overnight, using a rotating platform. Elution of deiminated (F95-bound) proteins was performed with the 4x non-denaturing elution buffer

according to the manufacturer's instructions (Merck), and the protein eluate was thereafter diluted 1:1 in 2 x Laemmli sample buffer (BioRad, UK), containing 5% beta-mercaptoethanol and boiled at 100°C for 5 min. Samples were thereafter kept frozen at -20 °C until further use for SDS-PAGE analysis, western blotting and in-gel digestion for LC-MS/MS analysis, as described below.

## **2.6 Western Blotting Analysis**

For western blotting, SDS-PAGE was carried out on the lamprey plasma and the corresponding isolated EV samples. All samples were diluted 1:1 in denaturing 2 x Laemmli sample buffer (containing 5 % beta-mercaptoethanol, BioRad, U.K.) and boiled for 5 min at 100 °C. Protein separation was carried out at 165 V for 50 min, using 4-20 % gradient TGX gels (BioRad U.K.), followed by western blotting at 15 V for 1 h using a Trans-Blot® SD semi-dry transfer cell (BioRad, U.K.). Membranes were stained with PonceauS (Sigma, U.K.) to assess even protein transfer and then blocked with 5 % bovine serum albumin (BSA, Sigma, U.K.) in Tris buffered saline (TBS) containing 0.1 % Tween20 (BioRad, U.K.; TBS-T) for 1 h at room temperature. Primary antibody incubation was carried out overnight at 4 °C on a shaking platform using the following antibodies: Anti-human PAD1 (ab181762, Abcam) PAD2 (ab50257 and ab16478), PAD3 (ab50246), PAD4 (ab50247) and PAD6 (PA5-72059, Thermo Fisher Scientific UK), all diluted 1/1000 in TBS-T, for the detection of a putative lamprey PAD-like protein via cross-reaction. The PAD2 antibody has been shown to cross react with a wide range of taxa and the PAD3 and PAD4 antibodies have also been shown to cross-react with PADs in other species (Lange et al., 2011; Lange et al., 2014; Magnadottir et al., 2018a and 2019a; Criscitiello et al., 2019 and 2020a,b; Pameneter et al., 2019; Phillips et al., 2020; Magnadottir et al., 2020; Bowden et al., 2020b). Plasma were further analysed for deiminated histone H3 (anti-citH3, ab5103, Abcam; diluted 1/1000), which is also used as an indicative marker of neutrophil extracellular trap formation (NETosis). For characterisation of plasma-EVs, two phylogenetically conserved EV-markers were used: CD63 (ab68418, Abcam; diluted 1/1000), and Flotillin-1 (ab41927, Abcam; diluted 1/1000). The nitrocellulose membranes were washed following primary antibody incubation at RT in TBS-T for 3 x 10 min and thereafter incubated with HRP-conjugated secondary antibodies (anti-rabbit IgG (BioRad), diluted 1/3000 in TBS-T), for 1h at RT. The membranes were washed for 5x10 min in TBS-T and digitally visualised, using enhanced chemiluminescence (ECL, Amersham, U.K.) in conjunction with the UVP BioDoc-ITTM System (Thermo Fisher Scientific, U.K.).

## **2.7 Silver Staining**

SDS-PAGE (using 4–20 % gradient TGX gels, BioRad, U.K.) was carried out under reducing conditions at 165 V for 50 min, for assessment of the F95-enriched protein eluates from whole plasma and plasma-EVs. The gels were silver stained according to the manufacturer's instructions, using the BioRad Silver Stain Plus Kit (1610449, BioRad, U.K.).

## **2.8 LC-MS/MS (Liquid Chromatography with Tandem Mass Spectrometry) Analysis of F95 Enriched Proteins**

Liquid chromatography with tandem mass spectrometry (LC-MS/MS) was carried out to identify deiminated protein candidates from lamprey plasma and plasma-EVs (pool of n=5 individual animals, respectively), according to previously described methods (Phillips et al., 2020; Criscitiello et al., 2020b). The LC-MS/MS analysis was carried out following in-gel digestion, with the F95-enriched protein preparations (diluted 1:1 in 2x Laemmli buffer and boiled for 5 min at 100°C) run 0.5 cm into

a 12 % TGX gel (BioRad, U.K.). The concentrated protein bands (containing the whole F95 eluate) were excised, trypsin digested and subjected to proteomic analysis using a Dionex Ultimate 3000 RSLC nanoUPLC (Thermo Fisher Scientific Inc, Waltham, MA, U.S.A.) system in conjunction with a QExactive Orbitrap mass spectrometer (Thermo Fisher Scientific Inc, Waltham, MA, U.S.A.), performed by Cambridge Proteomics (Cambridge, U.K.), as previously described (Bowden et al., 2020c; Criscitiello et al., 2020a). The data was processed post-run, using Protein Discoverer (version 2.1., Thermo Scientific) and MS/MS data were converted to mgf files which were submitted to the Mascot search algorithm (Matrix Science, London, U.K.) to identify deiminated protein hits. Search for F95 enriched proteins was conducted against a common UniProt database against Atlantic sea lamprey (*Petromyzon marinus*) CCP\_Petromyzon\_marinus\_20201214 (11407 sequences; 4607059 residues). An additional search was conducted against a common contaminant database (cRAP 20190401; 125 sequences; 41129 residues). The fragment and peptide mass tolerances were set to 0.1 Da and 20 ppm, respectively and the significance threshold value was set at of  $p < 0.05$  and a peptide cut-off score of 27 was applied (carried out by Cambridge Proteomics, Cambridge, U.K.).

## 2.9 Protein-Protein Interaction Network Analysis

To predict and identify functional protein-protein interaction networks associated to the deiminated proteins from lamprey plasma and plasma-EVs, STRING analysis (Search Tool for the Retrieval of Interacting Genes/Proteins; <https://string-db.org/>) was performed. Protein networks were generated based on protein names and applying the function of “search multiple proteins” in STRING (<https://string-db.org/>). Protein networks were built based on corresponding *Homo sapiens* protein identifiers as no species-specific protein database is available for lamprey in STRING. Furthermore, searching all Chordata protein databases in STRING, *Homo sapiens* showed the highest number of queries matched with the list of proteins identified here for lamprey. Parameters applied in STRING were as follows: “basic settings” and “medium confidence”. Colour lines connecting the nodes represent the following evidence-based interactions for the network edges: “known interactions” (these are based on experimentally determined curated databases), “predicted interactions” (these are based on gene neighbourhood, gene co-occurrence, gene fusion, via text mining, protein homology or co-expression). Gene ontology (GO) network clusters, Kyoto Encyclopedia of Genes and Genomes (KEEG) pathways and Reactome pathways for the deiminated protein networks were assessed in STRING and highlighted by colour coding (see the corresponding colour code keys showing the individual nodes and connective lines within each figure).

## 2.10 Statistical Analysis

NTA curves were generated using the Nanosight 3.0 software (Malvern, U.K.). The NTA curves show mean (black line) and standard error of mean (SEM), and the confidence intervals are indicated (red line). Protein-protein interaction networks were generated using STRING (<https://string-db.org/>), applying basic settings and medium confidence. Significance was considered as  $p \leq 0.05$ .

## 3. Results

### 3.1 Characterisation of Lamprey Plasma-EVs

The NanoSight NS300 was utilised for nanoparticle tracking analysis (NTA) of particle numbers and size distribution profiles of lamprey plasma-EVs. The EVs were poly-dispersed in the overall size range of 40-500 nm, with the majority of the EVs in the size range of 70-200 nm, and modal size of vesicles at 128-150 nm across the individual samples; an exemplar NTA curve is provided in Figure

1A. The lamprey EVs were positive for the two phylogenetically conserved EV-specific markers CD63 and Flot-1, as assessed by western blotting (Fig. 1B). Transmission electron microscopy (TEM) confirmed a poly-dispersed EV population (Fig. 1C), as observed by NTA analysis.

### 3.2 Deiminated Proteins and Putative PAD-like protein Detection in Lamprey Plasma

To assess the presence of putative deiminated proteins in lamprey plasma and plasma-EVs, the F95-enriched fractions were separated by SDS-PAGE and silver stained, revealing protein bands in sizes ranging between 10-250 kDa for plasma and 10-150 kDa for plasma-EVs, respectively (Figure 2A). The F95 enriched proteins were then further subjected to proteomic (LC-MS/MS) analysis revealing 48 deimination hits specific to whole plasma, 13 hits specific to plasma-EVs and further 24 overlapping hits. In addition, a number of non-characterised hits were found in both plasma and plasma-EVs, as represented in the Venn diagram in Fig. 2B and in Tables 1 and 2.

The anti-human PAD1, PAD2, PAD3, PAD4 and PAD6 antibodies were used for the assessment of a putative PAD-like protein in lamprey plasma, based on cross-reaction with human antibodies, using western blotting. A positive protein band at an expected approximate 70-75 kDa size was strongly detected using the anti-human PAD2 antibody on lamprey plasma, with a strong reaction also observed for the anti-human PAD6 antibody (where a double band was observed at 50 and 75 kDa), followed by the anti-human PAD3 antibody (at approximately 70-75 kDa) and the anti-human PAD1 antibody (a faint band at approximately 70-75 kDa), while no specific band was detected using the anti-human PAD4 antibody (Fig2C). The presence of deiminated histone H3 (citH3) was furthermore verified at the expected size of approximately 17 kDa in lamprey plasma (Fig. 2D). The sequence alignment of three previously reported PAD2-like amino acid sequences from lamprey showed that they all align the closest with teleost PAD-like proteins, followed by PAD-like protein from *Xenopus laevis*, and also group with the alligator PAD2 and human PAD2. Out of the human PAD isozymes, PAD6 grouped second closest with lamprey PADs, while PAD1, PAD3 and PAD4 were more distant in the tree (Fig. 2E). Furthermore, the three reported lamprey PAD2-like amino acid sequences showed 72-74% amino acid homology with each other and approximately 50.1- 50.6 % amino acid homology with human PAD2 and 49.8-51.6 % amino acid homology with sea bass PAD (Fig 2F; see also Supplementary Fig. 1 for percent identity matrix for all sequences in the phylogeny tree in Fig. 2E). To further assess if the human PAD2 antibody binds to a putative lamprey PAD in lamprey plasma, an immunoprecipitation was carried out, showing a dominant band at approximately 65-70 kDa following SDS-PAGE and silver staining of the IP fraction, while fainter bands around 50 kDa and 75 kDa were also observed (Supplementary Figure 2A). Furthermore, as the human PAD2 antibody is based on a peptide from aa 100-200 of the human PAD2 protein, sequence alignment of reported lamprey PAD-like protein sequences was performed, highlighting some conserved regions between the two species (Supplementary Figure 2B).

### 3.3 LC-MS/MS Analysis of Deiminated Proteins

Deiminated protein identification of F95 enriched proteins from lamprey plasma and plasma-EVs (pool from n=5 individuals, respectively) was carried out using LC-MS/MS analysis. Species-specific protein hits were identified using the UniProt lamprey database (Tables 1-2; see Supplementary Tables S1-S2 for detailed analysis). For plasma-EVs, a total of annotated 37 hits, whereof 13 protein hits were specific for EVs only were identified (Table 1). For plasma, 72 annotated hits were identified, whereof 48 were specific for plasma only (Table 2).

**Table 1.** Deiminated protein hits in plasma-EVs of lamprey (*P. marinus*) as identified by F95-enrichment in conjunction with LC-MS/MS analysis. Deiminated proteins were isolated from plasma-EVs by immunoprecipitation using the pan-deimination F95 antibody. The resulting F95-enriched eluate was then analysed by LC-MS/MS and peak list files submitted to Mascot, using the species-specific UniProt lamprey (*P. marinus*) database. Peptide sequence hits are listed, showing match and number of sequences for individual protein hits and total score (see further detailed analysis in Supplementary Table S1). \*Proteins only identified in plasma-EVs are highlighted in orange.

Protein ID Protein Name	Matches (Sequences)	Total score ( $p < 0.05$ ) <sup>†</sup>
<b>ALBU_PETMA</b> Serum albumin SDS-1	19 (14)	661
<b>S4RXQ3_PETMA</b> Uncharacterized protein	17 (13)	613
<b>S4RBZ1_PETMA</b> SERPIN domain-containing protein	44 (9)	548
<b>S4RH70_PETMA</b> DUF1081 domain-containing protein	16 (15)	539
<b>S4RH85_PETMA</b> Uncharacterized protein (Beta-actin; Actin gamma 2, smooth muscle)	7 (5)	248
<b>*S4RE82_PETMA</b> Desmin b	6 (4)	191
<b>S4RFV4_PETMA</b> Uncharacterized protein	4 (3)	180
<b>*S4RBJ3_PETMA</b> 60 kDa chaperonin	2 (2)	147
<b>APL2_PETMA</b> Blood plasma apolipoprotein LAL2	4 (2)	144
<b>S4RPV0_PETMA</b> Fibrinogen C-terminal domain-containing protein	8 (4)	138
<b>S4RP12_PETMA</b> Plastocyanin-like domain-containing protein	12 (3)	137
<b>S4RB03_PETMA</b> Histone H2B	9 (4)	137
<b>S4RAY0_PETMA</b> Histone H4	8 (3)	135
<b>S4S091_PETMA</b> C1q domain-containing protein	4 (3)	101
<b>S4S090_PETMA</b> C1q domain-containing protein	5 (2)	92
<b>S4S165_PETMA</b> Histone H2A	4 (2)	86
<b>*S4RIP9_PETMA</b> 78 kDa glucose-regulated protein	3 (2)	81
<b>S4R4V3_PETMA</b> Pyruvate kinase	2 (2)	77
<b>S4RVPO_PETMA</b> Anaphylatoxin-like domain-containing protein	2 (2)	70
<b>*S4RFB7_PETMA</b> 60S ribosomal protein L23	5 (1)	69
<b>S4RGP3_PETMA</b> Uncharacterized protein	1 (1)	68
<b>S4S1N9_PETMA</b> Elongation factor 1-alpha	2 (1)	58
<b>* S4RX19_PETMA</b> Septin 7	1 (1)	56

<b>S4RR08_PETMA</b> 2-phospho-D-glycerate hydro-lyase	1 (1)	53
<b>S4R8Z6_PETMA</b> C1q and TNF related 9	2 (1)	51
<b>S4RDV2_PETMA</b> Heat shock protein 90, alpha (cytosolic), class A member 1, tandem duplicate 2	1 (1)	48
<b>S4RL04_PETMA</b> Tyrosine 3-monooxygenase/tryptophan 5-monooxygenase activation protein eta	1 (1)	46
<b>S4RAY6_PETMA</b> Histone H3	2 (1)	46
<b>*S4RRG5_PETMA</b> 160 kDa neurofilament protein	2 (1)	44
<b>S4RNE3_PETMA</b> 60S ribosomal protein L18a	1 (1)	43
<b>*S4RWRO_PETMA</b> 60S ribosomal protein L8	2 (1)	43
<b>*S4S171_PETMA</b> 60S acidic ribosomal protein P0	1 (1)	39
<b>S4RID2_PETMA</b> Uncharacterized protein (Fibrinogen C-terminal domain- containing protein)	1 (1)	37
<b>*S4R4R6_PETMA</b> Ribosomal protein L3 like	1 (1)	36
<b>*S4RPS8_PETMA</b> 75 kDa glucose-regulated protein	2 (1)	36
<b>*S4RCL1_PETMA</b> OTU deubiquitinase with linear linkage specificity b	4 (1)	35
<b>S4RZ58_PETMA</b> CRAL-TRIO domain-containing protein	1 (1)	35
<b>*S4RDIO_PETMA</b> FACT complex subunit	3 (1)	34
<b>S4S0H1_PETMA</b> Uncharacterized protein	1 (1)	32
<b>S4R9Q9_PETMA</b> Peptidase S1 domain-containing protein	1 (1)	30
<b>S4RYF8_PETMA</b> Gp_dh_N domain-containing protein	2 (1)	30
<b>*S4S068_PETMA</b> Spartin b	2 (1)	27

† Ions score is  $-10 \cdot \log(P)$ , where P is the probability that the observed match is a random event. Individual ions scores > 27 indicate identity or extensive homology ( $p < 0.05$ ). Protein scores are derived from ions scores as a non-probabilistic basis for ranking protein hits.

**Table 2.** Deiminated protein hits in lamprey (*P. marinus*) whole plasma, as identified by F95-enrichment in conjunction with LC-MS/MS analysis. Deiminated proteins were isolated from plasma (n=5) by immunoprecipitation using the pan-deimination F95 antibody. The resulting F95-enriched eluate was then analysed by LC-MS/MS and peak list files submitted to Mascot, using the lamprey (*P. marinus*) UniProt database. Peptide sequence hits are listed, showing matches and sequences for protein hits and total score (see further detailed analysis in Supplementary Table S2). \*Proteins only identified in whole plasma are highlighted in blue.

Protein ID Protein Name	Matches (Sequences)	Total score ( $p < 0.05$ ) <sup>†</sup>
----------------------------	------------------------	--

<b>S4RH70_PETMA</b> DUF1081 domain-containing protein	155 (130)	8035
<b>ALBU_PETMA</b> Serum albumin SDS-1	177 (77)	4663
<b>S4RXQ3_PETMA</b> Uncharacterized protein	73 (47)	2757
<b>S4RFV4_PETMA</b> Uncharacterized protein	46 (36)	2216
<b>*S4RQ55_PETMA</b> Uncharacterized protein	21 (21)	1175
<b>S4RBZ1_PETMA</b> SERPIN domain-containing protein	123 (15)	1085
<b>*S4RJX5_PETMA</b> Uncharacterized protein	21 (15)	943
<b>S4RVPO_PETMA</b> Anaphylatoxin-like domain-containing protein	17 (13)	899
<b>*S4RPC4_PETMA</b> Fibrinogen beta chain	17 (13)	834
<b>S4RP12_PETMA</b> Plastocyanin-like domain-containing protein	45 (14)	810
<b>*FIBG_PETMA</b> Fibrinogen gamma chain	18 (14)	753
<b>*S4REY0_PETMA</b> Activation peptide fragment 1	15 (10)	747
<b>*K7N848_PETMA</b> Angiotensinogen	13 (11)	732
<b>*S4RGTO_PETMA</b> Uncharacterized protein	16 (12)	717
<b>S4RUQ3_PETMA</b> SERPIN domain-containing protein	18 (13)	710
<b>S4RGP3_PETMA</b> Uncharacterized protein	13 (11)	704
<b>S4RPV0_PETMA</b> Fibrinogen C-terminal domain-containing protein	19 (11)	689
<b>*S4RUS7_PETMA</b> Serp peptidase inhibitor, clade D (heparin cofactor), member 1	13 (11)	669
<b>*S4RC14_PETMA</b> Fibronectin	12 (12)	656
<b>S4RID2_PETMA</b> Uncharacterized protein	15 (8)	594
<b>*S4RSU9_PETMA</b> Albumin domain-containing protein	16 (11)	511
<b>S4R8Z6_PETMA</b> C1q and TNF related 9	11 (8)	511
<b>S4RSZ0_PETMA</b> Fibrinogen C-terminal domain-containing protein	10 (8)	455
<b>*S4RQ61_PETMA</b> Uncharacterized protein	9 (8)	454
<b>*O42160_PETMA</b> Trypsinogen b2	12 (6)	433
<b>S4RVH9_PETMA</b> Peptidase S1 domain-containing protein	12 (6)	424
<b>*S4RQD7_PETMA</b> Uncharacterized protein	6 (6)	381
<b>S4RH85_PETMA</b> Uncharacterized protein (Beta-actin; Actin gamma 2, smooth	6 (6)	347

muscle)		
<b>*FIBA1_PETMA</b> Fibrinogen alpha-1 chain	5 (4)	346
<b>*S4RT32_PETMA</b> Adiponectin, C1Q and collagen domain containing	7 (5)	339
<b>*S4R568_PETMA</b> Tubulin beta chain	7 (6)	334
<b>S4S1D7_PETMA</b> Glyceraldehyde-3-phosphate dehydrogenase	5 (5)	331
<b>S4RL04_PETMA</b> Tyrosine 3-monooxygenase/tryptophan 5-monooxygenase activation protein eta	6 (6)	308
<b>APL2_PETMA</b> Blood plasma apolipoprotein LAL2	6 (5)	295
<b>*S4RW10_PETMA</b> Ferritin	4 (4)	295
<b>*LDH_PETMA</b> L-lactate dehydrogenase	4 (4)	272
<b>S4RJ23_PETMA</b> C1q and TNF related 9	6 (5)	270
<b>*S4S0L1_PETMA</b> Jacalin-type lectin domain-containing protein	6 (6)	258
<b>*S4R963_PETMA</b> Cytoglobin	4 (4)	248
<b>S4RB03_PETMA</b> Histone H2B	9 (5)	246
<b>*S4RUX0_PETMA</b> Ferritin	4 (4)	238
<b>S4R4V3_PETMA</b> Pyruvate kinase	7 (4)	237
<b>S4*RR00_PETMA</b> TED_complement domain-containing protein	5 (4)	228
<b>*S4RWE8_PETMA</b> M20_dimer domain-containing protein	4 (4)	211
<b>S4RAY0_PETMA</b> Histone H4	4 (4)	209
<b>S4S1N9_PETMA</b> Elongation factor 1-alpha	4 (4)	188
<b>*S4RMH3_PETMA</b> Ferritin	4 (4)	165
<b>S4S090_PETMA</b> C1q domain-containing protein	21 (2)	163
<b>S4RAZ5_PETMA</b> Histone H2A	3 (3)	154
<b>*S4RLF1_PETMA</b> Alpha-1,4 glucan phosphorylase	3 (3)	139
<b>S4S088_PETMA</b> C1q domain-containing protein	3 (2)	130
<b>*S4RFY7_PETMA</b> Jacalin-type lectin domain-containing protein	3 (3)	127
<b>S4RDV2_PETMA</b> Heat shock protein 90, alpha (cytosolic), class A member 1, tandem duplicate 2	2(2)	123
<b>*S4RDR7_PETMA</b> Uncharacterized protein	3 (3)	121
<b>*S4R694_PETMA</b>	3	118

Triosephosphate isomerase	(3)	
<b>*S4R691_PETMA</b> AMP deaminase	3 (3)	118
<b>*S4RTN2_PETMA</b> Zgc:152830	3 (3)	116
<b>*S4RGR5_PETMA</b> Fructose-bisphosphate aldolase	2 (2)	115
<b>*S4RXJ5_PETMA</b> Carnosine dipeptidase 2	2 (2)	109
<b>S4RG79_PETMA</b> C1q domain-containing protein	3 (2)	105
<b>S4RG79_PETMA</b> 2-phospho-D-glycerate hydro-lyase	1 (1)	104
<b>S4RX00_PETMA</b> N-glycanase_N domain-containing protein	2 (2)	102
<b>S4RQ44_PETMA</b> PFK domain-containing protein	1 (1)	102
<b>S4RWRO_PETMA</b> 60S ribosomal protein	4 (2)	99
<b>S4S092_PETMA</b> C1q domain-containing protein	3 (2)	98
<b>*S4RQL1_PETMA</b> Ribosomal protein L7	2 (2)	96
<b>S4S165_PETMA</b> Histone H2A	2 (2)	92
<b>S4R6W7_PETMA</b> C1q domain-containing protein	2 (2)	83
<b>*S4RPI3_PETMA</b> 60S ribosomal protein L13a	1 (1)	77
<b>S4S0H1_PETMA</b> Uncharacterized protein	1 (1)	76
<b>S4RE39_PETMA</b> Peptidase S1 domain-containing protein	2 (2)	73
<b>*S4R718_PETMA</b> Ribosomal protein L4	2 (2)	72
<b>*S4RXD9_PETMA</b> Carbonic anhydrase	1 (1)	72
<b>*S4RFI6_PETMA</b> Ribosomal protein L23a	1 (1)	68
<b>*S4R5M7_PETMA</b> 3-hydroxyacyl-[acyl-carrier-protein] dehydratase	1 (1)	62
<b>S4RW50_PETMA</b> C1q and TNF related 9	1 (1)	58
<b>*S4RAY9_PETMA</b> H15 domain-containing protein	1 (1)	57
<b>*S4RJV6_PETMA</b> Uncharacterized protein	2 (2)	56
<b>*S4RQ52_PETMA</b> Uncharacterized protein	1 (1)	56
<b>*S4RXC9_PETMA</b> Uncharacterized protein	1 (1)	50
<b>S4RZ58_PETMA</b> CRAL-TRIO domain-containing protein	2 (2)	47
<b>S4RAY6_PETMA</b> Histone H3	1 (1)	47
<b>*S4R900_PETMA</b>	1	45

Erythrocyte membrane protein band 4.1 like 2	(1)	
<b>*S4R4U3_PETMA</b> 40S ribosomal protein S9	1 (1)	41
<b>*S4RV01_PETMA</b> 40S ribosomal protein S11	1 (1)	40
<b>*S4RLF4_PETMA</b> Cap methyltransferase 1	1 (1)	40
<b>*S4RZY7_PETMA</b> Olfactomedin 4	1 (1)	36
<b>*S4RW45_PETMA</b> Uncharacterized protein	2 (1)	35
<b>*S4RV41_PETMA</b> PLAT domain-containing protein	2 (1)	34
<b>*S4RFJ2_PETMA</b> Ankyrin repeat domain 28	1 (1)	33
<b>S4RFF9_PETMA</b> 60S ribosomal protein L18a	1 (1)	32
<b>*S4RXZ4_PETMA</b> Centromere protein S	2 (1)	32
<b>*S4RQC8_PETMA</b> Uncharacterized protein	1 (1)	30
<b>*S4RIK4_PETMA</b> Kringle domain-containing protein	1 (1)	30
<b>*S4RVF7_PETMA</b> Glutamine-fructose-6-phosphate transaminase	1 (1)	30
<b>*S4RVF7_PETMA</b> 40S ribosomal protein S26	1 (1)	29
<b>*S4RU19_PETMA</b> Protein kinase domain-containing protein	2 (1)	29
<b>*S4RZ42_PETMA</b> 60S ribosomal protein L21	1 (1)	29
<b>*S4RCX7_PETMA</b> Fibrinopeptide A	1 (1)	29
<b>*S4RHB4_PETMA</b> KIF-binding protein	1 (1)	28
<b>*S4R6P0_PETMA</b> Uncharacterized protein	2 (1)	28
<b>*S4R9C6_PETMA</b> DDE_Tnp_1_7 domain-containing protein	1 (1)	27
<b>*S4RH55_PETMA</b> LRRNT domain-containing protein	1 (1)	27
<b>*S4RXB2_PETMA</b> Palmitoyltransferase	1 (1)	27
<b>*S4R9Z3_PETMA</b> Anoctamin	1 (1)	27
<b>*S4RDD9_PETMA</b> Vesicle-fusing ATPase	1 (1)	26
<b>*S4RUU5_PETMA</b> Myosin motor domain-containing protein	1 (1)	26

† Ions score is  $-10 \cdot \log(P)$ , where P is the probability that the observed match is a random event. Individual ions scores > 27 indicate identity or extensive homology ( $p < 0.05$ ). Protein scores are derived from ions scores as a non-probabilistic basis for ranking protein hits.

### 3.4 Functional Protein Interaction Networks for Deiminated Proteins in Lamprey

To predict protein-protein interaction networks for deiminated protein hits identified in lamprey plasma and plasma-EVs, the protein names were submitted to STRING (Search Tool for the Retrieval of Interacting Genes/Proteins) analysis (<https://string-db.org/>). Protein interaction networks were based on known and predicted interactions and represent all deiminated proteins identified in lamprey and their interaction partners present in the STRING database, based on networks for human (*Homo sapiens*). A lamprey-specific protein database is not available in STRING, and the human protein database showed, out of all Chordata, the highest number of queries matched with the lamprey protein list for deiminated hits.

#### **3.4.1 Protein interaction network analysis for deiminated proteins in lamprey plasma-EVs**

For deiminated protein hits identified in plasma-EVs, the PPI enrichment  $p$ -value was  $1.28 \times 10^{-11}$ , indicating more significant interactions than expected for a similar sized group of unrelated proteins (Fig 3A). STRING network cluster analysis showed enrichment in pathways for: Peptide chain elongation, Viral mRNA translation, Glycolysis and gluconeogenesis, Cellular response to heat stress, Muscle protein and striated muscle thin filament, Nucleosome, Protein processing in endoplasmic reticulum; and Nucleosome and histone deacetylase complex (Fig 3B). KEGG pathways identified to be enriched for deiminated proteins in the EVs were: RNA degradation, Ribosome, Antigen processing and presentation, Glycolysis/Gluconeogenesis, Biosynthesis of amino acids, Thyroid hormone synthesis, Complement and coagulation cascade (Fig 3C); as well as Prion diseases, Arrhythmogenic right ventricular cardiomyopathy (ARVC), *Staphylococcus aureus* infection, Hypertrophic cardiomyopathy, Legionellosis, Dilated Cardiomyopathy, Fluid shear stress and atherosclerosis (Fig 3D). Molecular GO pathways identified for the deiminated protein hits in the EVs were: Unfolded protein binding, Structural constituent of ribosome, rRNA binding, Chaperone binding, Structural constituent of cytoskeleton, Ubiquitin protein ligase binding, Histone binding, Structural molecule activity, Identical protein binding, Purine ribonucleoside triphosphate binding (Fig 3E); as well as Purine ribonucleotide binding, ATP binding, Carbohydrate derivative binding, Drug binding, Anion binding, Enzyme binding, Small molecule binding, Protein binding and Heterocyclic compound binding (Fig 3F). Furthermore, Reactome network analysis for the deiminated protein hits of lamprey plasma-EVs included pathways for: Infectious disease, Post-translational protein phosphorylation, Axon guidance, MAPK family signalling cascades, Disease, Hemostasis, Innate immune system, Metabolism of proteins, Immune system, Metabolism (Fig 3G); as well as Influenza viral RNA transcription and replication, Cellular response to heat stress, Regulation of complement cascade, Mitochondrial protein import, Regulation of actin dynamics for phagocytic cup formation, Regulation of HSF1-mediated heat shock response, Major pathway of rRNA processing in the nucleus and cytoplasm, Platelet degranulation, VEGFA-VEGFR2 Pathway, Nonsense mediated decay (NMD) enhanced by the exon junction (Fig 3H); and Reactome pathways for Scavenging by class F receptors, HSF1 activation, Binding and uptake of ligands by scavenger receptors Peptide chain elongation, Plasma lipoprotein remodelling, Viral nRNA translation, Eukaryotic translation termination, Selenocysteine synthesis, Nonsense mediated decay (NMD) independent of the exon, MAPK2 and MAPK activation (Fig 3I).

#### **3.4.2 Protein interaction network analysis for deiminated proteins in lamprey plasma**

For deiminated proteins identified in whole lamprey plasma, the PPI enrichment  $p$ -value was  $2.78 \times 10^{-15}$ , which is indicative of significantly more interactions than expected for a similar sized set of unrelated proteins (Fig 4A). Local STRING network analysis identified enrichment for: Adipokinetic hormone receptor activity, Fibrinogen alpha/beta chain family, peptidase S1A, Glutathione synthesis and recycling- arginine, Fructose 1,6-bisphosphate metabolic process, Glycolysis and gluconeogenesis, Viral mRNA translation, Peptide chain elongation, Carbon metabolism and lactate dehydrogenase activity, Post-translational protein phosphorylation, Regulation of insulin-like growth factor transport and clotting cascade (Fig 4B). KEGG pathway identified were: Glycolysis/gluconeogenesis, Ribosome, Biosynthesis of amino acids, Fructose and mannose metabolism, Carbon metabolism, Complement and coagulation cascades, HIF-1 signalling pathway, Platelet activation, Influenza A, Type II diabetes mellitus (Fig 4C). Molecular GO pathways identified were: Structural constituent of ribosome, rRNA binding, Hydro-lyase activity, Lyase activity, Structural molecule activity and Identical protein binding (Fig 4D).

### **3.4.3 Common and specific protein interaction networks for deiminated proteins in lamprey plasma and plasma-EVs, respectively**

Common STRING network clusters for deiminated proteins in plasma and plasma-EVs were transcriptional, immune and metabolic related and included: Peptide chain elongation, Viral mRNA translation, Glycolysis and gluconeogenesis.

STRING network clusters specific for deiminated proteins in EVs only related to immune, metabolic and gene regulatory pathways and were: Cellular response to heat stress, Muscle protein and striated muscle thin filament, Nucleosome, Protein processing in endoplasmic reticulum, Nucleosome and histone deacetylase complex.

STRING network clusters specific for deiminated proteins in plasma only were associated to immune and metabolic functions and included: Fibrinogen alpha/beta chain family, Adipokinetic hormone receptor activity, peptidase S1A, Glutathione synthesis and recycling- arginine, Fructose 1,6-bisphosphate metabolic process, Carbon metabolism and lactate dehydrogenase activity, Post-translational protein phosphorylation, Regulation of insulin-like growth factor transport and clotting cascade.

Common KEGG pathways for deiminated proteins in plasma and plasma-EVs included were: Complement and coagulation cascade, Ribosome, Glycolysis/Gluconeogenesis and Biosynthesis of amino acids

KEGG pathways identified to be enriched for deiminated proteins in the lamprey EVs only were: Antigen processing and presentation, *Staphylococcus aureus* infection, Legionellosis, Prion diseases, Fluid shear stress and atherosclerosis, RNA degradation, Thyroid hormone synthesis, Arrhythmogenic right ventricular cardiomyopathy (ARVC), Hypertrophic cardiomyopathy, Dilated Cardiomyopathy.

KEGG pathway identified for deiminated proteins in whole plasma only were: HIF-1 signalling pathway, Platelet activation, Influenza A, Fructose and mannose metabolism, Carbon metabolism, Type II diabetes mellitus.

Common Molecular function GO pathways for deiminated proteins in plasma and plasma-EVs were: Structural constituent of ribosome, rRNA binding, Identical protein binding, Structural molecule activity.

Molecular function GO pathways identified for deimination hits in the EVs were: Unfolded protein binding, Chaperone binding, Structural constituent of cytoskeleton, Ubiquitin protein ligase binding, Histone binding, Purine ribonucleoside triphosphate binding, Purine ribonucleotide binding, ATP binding, Carbohydrate derivative binding, Drug binding, Anion binding, Enzyme binding, Small molecule binding, Protein binding and Heterocyclic compound binding.

Molecular function GO pathways identified for deiminated proteins in whole plasma only were: Hydro-lyase activity, Lyase activity.

When assessing Reactome pathways, interestingly a far higher number of pathways were identified for the deiminated protein hits in the EVs, compared with deiminated hits in whole plasma. Only two Reactome pathways were identified by STRING analysis for deiminated proteins in whole plasma: Metabolism and Developmental biology, whereof the Metabolism pathway was common with EVs. Developmental biology pathway was specific to whole plasma only. An additional 29 Reactome pathways were identified for deiminated proteins in EVs, these included: Infectious disease, Disease, Immune system, Innate immune system, Influenza viral RNA transcription and replication, Scavenging by class F receptors, Binding and uptake of ligands by scavenger receptors, Viral nRNA translation, Cellular response to heat stress, Regulation of complement cascade, Heat shock factor 1 (HSF1) activation, Regulation of HSF1-mediated heat shock response, Regulation of actin dynamics for phagocytic cup formation, Hemostasis, Platelet degranulation, VEGFA-VEGFR2 Pathway, Post-translational protein phosphorylation, Axon guidance, MAPK family signalling cascades, MAPK2 and MAPK activation, Major pathway of rRNA processing in the nucleus and cytoplasm, Nonsense mediated decay (NMD) enhanced by the exon junction, Nonsense mediated decay (NMD) independent of the exon, Peptide chain elongation, Eukaryotic translation termination, Selenocysteine synthesis, Plasma lipoprotein remodelling, Metabolism of proteins and Mitochondrial protein import.

The Venn diagram in Fig. 5 summarises the number of specific and overlapping STRING network cluster, KEGG pathways, Molecular GO pathways and Reactome pathways identified for deiminated protein hits in lamprey plasma (“plasma citrullinome”) and plasma-EVs (“EV citrullinome”).

#### 4. Discussion

The current study verified the presence of PAD-like protein in lamprey plasma, characterised deimination signatures in plasma and plasma-EVs, and furthermore provides the first characterisation of plasma-EVs from lamprey.

Sea lamprey plasma-EVs showed a poly-dispersed population in the range of 40-500 nm, with modal sizes at 128-150 nm and with the main amount of EVs falling within 70-200 nm. While in most species, EV NTA profiles fall overall within a 50-600 nm range, some species specific differences in EV size distribution profiles can be observed. For example, in teleost fish sera EVs have been seen to vary between species, cod serum-EVs were found at 50-300 nm size range (Magnadottir et al., 2020a), while EVs profiles of halibut sera were 50-600 nm (Magnadottir et al., 2021). Nurse shark

plasma-EVs were observed at sizes mainly 20-200 nm (Criscitiello et al., 2019), similar as seen here in sea lamprey, while EV hemolymph profiles of different Mollusca species varied between a 30-300 nm range in some and 90-500 nm range in others (Bowden et al., 2020c). In marine mammals, pinniped serum-EVs were observed at 50-600 nm (Magnadottir et al., 2020c), while in cetaceans serum-EVs were observed at 50-500 nm size range or at narrower ranges of 90-300 nm, depending on species (Magnadottir et al., 2020b). Lamprey plasma-EVs were here found to be strongly positive both for CD63, a marker for small EVs (“exosomes”, <100 nm) and for flotillin-1, a marker for medium or larger EVs (“microvesicles”; 100-1000 nm), and this corresponds with the size distribution profiles observed by NTA, as well as with the poly-dispersed EV population seen by TEM. Lamprey EV characterisation in the current study therefore meets the requirements for the characterisation of EVs according to the minimal information for studies of extracellular vesicles of the International Society for Extracellular Vesicles (MISEV; Théry et al., 2018). Flotillin-1 has indeed been characterised in lamprey and confirmed as a putative marker for EVs (Xu et al., 2017). In Japanese lampren/Arctic lamprey (*Lampetra japonica*), EVs have previously been isolated from conditioned growth medium of primary supraneural myeloid body cells (SMB cells) and suggested to play immune modulating roles in response to LPS stimulation (Wang et al., 2019a). The current study is though the first to characterise EVs from lamprey plasma.

In the current study, putative PAD-like protein was detected in lamprey plasma via cross-reaction using human PAD antibodies, with the strongest reactivity observed against the anti-human PAD2 antibody, showing a protein band at expected size for PAD2 (at approximately 70-75 kDa). Positive detection in lamprey plasma via cross-reaction with the anti-human PAD antibodies correlates with that PAD2-like protein sequences have previously been reported in lamprey (XP\_032825558.1; XP\_032825490.1; XP\_032825520.1), while immunoprecipitation of lamprey plasma with the human PAD2 antibody revealed both a dominant 65-70 kDa band and additional bands (at 50 and 75 kDa). While the human antibody is raised against a peptide sequence of aa 100-200 of human PAD2 and there is a considerable number of conserved amino acids in this region between human and lamprey (see Supplementary Figure 2B), it may be possible that protein conformational differences in Western blotting versus IP application lead to some differences in protein band detection between the two assays. Antibodies against human PAD1, 3, 4 and 6 were also assessed on lamprey plasma, showing the second strongest cross-reaction with the PAD6 antibody, followed by the PAD3 and PAD1 antibodies, all detecting bands around the expected size for PADs at 70-75 kDa; while negligible cross reaction was observed for the PAD4 antibody. This corresponded overall with the amino acid sequence alignment for the three reported PAD2-like protein sequences from lamprey, which showed that the lamprey PAD2-like proteins all align most closely with human PAD2 and teleost PADs; notably in bony fish only PAD2-like form has been described and PAD2 is considered the most phylogenetically conserved PAD isozyme (Rebl et al., 2010; Magnadottir et al., 2018a). This was then followed by similarity to protein sequences for human PAD6, while human PAD4, PAD3 and PAD1 were more distant in the tree. Furthermore, the three lamprey PAD2-like proteins showed 72-74% amino acid identity with each other and approximately 50.1- 50.6 % amino acid identity with human PAD2 and 49.8-55.2 % amino acid identity with reported teleost (sea bass and rainbow trout) PADs. While the current study provides some evidence for cross-reaction between human PAD antibodies and lamprey PADs, further studies on PADs in lamprey will require the generation of lamprey specific PAD antibodies. Indeed, as the field of PAD research is still very limited regarding tools, including in human studies, the generation of species-specific antibodies will be paramount in

supporting further in depth investigations for the diverse roles of PADs in other species; including in comparative animal models of human pathologies.

Using Western blotting, the presence of deiminated histone H3 was detected with a commercially available citH3 specific antibody which is predicted to react with a range of species, and has previously been assessed in a range of taxa including teleost and cartilaginous fish, reptile, bird and mammals (Magnadottir et al., 2018a; Magnadottir et al., 2019a; Criscitiello et al., 2019; Criscitiello et al., 2020b; Lange et al., 2011; Criscitiello et al., 2020a). In sea lamprey plasma a band at the expected ~17 kDa size was detected for citH3 and the presence of histone H3 in deiminated form was furthermore confirmed in the LC-MS/MS analysis of F95 enriched lamprey proteins. While histone deimination plays roles in gene regulatory events, histone H3 deimination is also a recognised marker for extracellular trap formation (NET/ETosis), where chromatin nets are cast from neutrophils to capture pathogens that are too large for phagocytosis, and this has been identified across phyla (Brinkmann et al., 2004; Palić et al., 2007; Claushuis et al., 2018; Deng et al., 2020; Zuo et al., 2020). Trap formation has not been reported in lamprey to our knowledge and via the detection of citH3 here, signs of ET/NETosis are therefore identified for the first time in lamprey. The assessment of NETosis in response to various pathogen stimuli, which may also drive different NETosis pathways, including PAD-mediated NETosis (Konig and Adrade, 2016; Vorobjeva and Chernyak, 2020), will require further in depth functional analysis, for example using lamprey leukocyte *in vitro* assays and a range of stimuli.

A proteomic approach was used to identify deiminated proteins by F95 enrichment in conjunction with LC-MS/MS analysis, in both plasma-EVs as well as whole plasma. Deiminated target proteins identified by this method related to various immune, metabolic and gene regulatory pathways and showed differences between plasma-EVs, versus whole plasma, while some deimination targets were overlapping. As deimination contributes to the moonlighting abilities of proteins it is of considerable interest how this post-translational modification may contribute to the multifaceted function of target proteins, including under physiological conditions. This is furthermore interesting as PAD isozyme diversification is greater in mammals (five PAD isozymes) while fewer PAD isozymes are identified in non-mammalian vertebrates (three in reptiles and birds, one in fish). The different human PAD isozymes have been shown to display different preferences for protein targets, with PAD2 for example having a broader range of target proteins compared with PAD4 (Bicker and Thompson, 2013). Furthermore, the different PAD isozymes have tissue specific expression, with PAD2 being the most ubiquitously expressed isoform with the widest range of target proteins, while in teleost fish and in lampreys there is only PAD2-like protein reported, which is presumably responsible for all protein deimination. It may be possible that conserved PAD-mediated deimination contributes to the diversification of multiple protein pathways throughout phylogeny, including those of the immune system. In lamprey plasma, functional protein-protein interaction network analysis for gene ontology (GO) and KEGG pathways identified both common and specific pathways for the deiminated protein hits in EVs and plasma respectively, and these are discussed below.

Building protein interaction networks for deimination signatures in lamprey plasma and plasma-EVs, using the human database, as no lamprey specific database is available in STRING, revealed local STRING network clusters, KEGG, Molecular GO pathways and Reactome pathways, some of which overlapped and some of which were specific to either whole plasma or plasma-EVs, as summarised in the Venn diagram in Fig. 5.

Findings for deimination enrichment in protein-protein interaction networks, including in KEEG pathways, in lamprey plasma and plasma-EVs showed some similarity to findings from previous studies in other taxa. Common KEEG pathways for deiminated proteins in plasma and plasma-EVs included were: Complement and coagulation cascade, Ribosome, Glycolysis/Gluconeogenesis and Biosynthesis of amino acids. Both complement and coagulation cascades, as well as biosynthesis of amino acids pathways have previously been identified as deimination enriched KEEG pathways in plasma and plasma-EVs of bovine (Criscitiello et al., 2020c), reindeer (D'Alessio et al., 2021) and naked mole-rat (Pamenter et al., 2019). The complement KEEG pathway has furthermore been identified to be deiminated in pelagic seabird plasma (Phillips et al., 2020) and in horseshoe crab (Bowden et al., 2020a). The ribosome KEEG pathway has been identified in alligator EVs, alongside glycolysis/gluconeogenesis pathway (Criscitiello et al., 2020b), which has also been identified as deiminated in naked mole-rat EVs (Pamenter et al., 2019), in horseshoecrab and lobster haemolymph (Bowden et al., 2020a,b) and in cetacean sera (Magnadottir et al., 2020). The biosynthesis of amino acids KEEG pathway was previously identified as deiminated in alligator EVs (Criscitiello et al., 2020) and in lobster haemolymph (Bowden et al., 2020).

KEEG pathways identified to be enriched for deiminated proteins in the lamprey EVs only were: Antigen processing and presentation, *Staphylococcus aureus* infection, Legionellosis, Prion diseases, Fluid shear stress and atherosclerosis, RNA degradation, Thyroid hormone synthesis, Arrhythmogenic right ventricular cardiomyopathy ARVC), Hypertrophic cardiomyopathy, Dilated Cardiomyopathy. Some of these pathways have been identified either in plasma/serum or EVs in various other species. This includes the *S.aureus* KEEG pathway in naked mole-rat plasma and plasma-EVs (Pamenter et al., 2019), in pelagic seabird plasma (Phillips et al., 2020), in cetacean sera (Magnadottir et al., 2020), in reindeer EVs (D'Alessio et al., 2021) and in horseshoecrab haemolymph (Bowden et al., 2020a). The prion disease KEEG pathway has been found deiminated in naked mole-rat and reindeer-EVs, as well as in bovine plasma and plasma-EVs (Criscitiello et al., 2020c), in albatross (*Diomedea exulans*) plasma (Phillips et al., 2020) and cetacean sera (Magnadottir et al., 2020). Thyroid hormone synthesis has been identified as a deiminated KEEG pathway in reindeer plasma (D'Alessio et al., 2021) and in cetacean sera (Magnadottir et al., 2020). Cardiomyopathy KEEG pathways have also been identified as deiminated in relation to viral myocarditis in bovine deimination enrichment networks (Criscitiello et al., 2020c).

KEEG pathway identified for deiminated proteins in whole plasma only were: HIF-1 signalling pathway, Platelet activation, Influenza A, Fructose and mannose metabolism, Carbon metabolism, Type II diabetes mellitus. The HIF-1 KEEG pathway has been previously identified as deimination enriched in cetacean sera (Magnadottir et al., 2020) and naked mole-rat plasma-EVs (Pamenter et al., 2019). The platelet activation KEEG pathway has been identified as deiminated in reindeer plasma-EVs (D'Alessio et al., 2021) and the carbon metabolism KEEG pathway in horseshoecrab and lobster haemolymph (Bowden et al., 2020a,b).

The individual protein hits identified to be deiminated showed a number of common targets in whole plasma and plasma-EVs, while other deimination targets were only found in EVs. These target proteins of deimination relate directly to the functional protein-networks presented in Figures 3 and 4.

Common deiminated protein targets in plasma and plasma-EVs included: fibrinogen C-terminal-domain containing protein, C1q domain-containing protein, C1q and TNF related 9, Anaphylatoxin-like domain-containing protein, SERPIN domain-containing protein, DUF1081 domain-containing protein, Blood plasma apolipoprotein LAL2, Serum albumin, Plastocyanin-like domain-containing protein, Beta-actin; Actin gamma 2, Elongation factor 1-alpha, Pyruvate kinase, Histone H2A, Histone H2B, Histone H3, Histone H4, 2-phospho-D-glycerate hydro-lyase, Heat shock protein 90, Glyceraldehyde-3-phosphate dehydrogenase, Tyrosine 3-monooxygenase/tryptophan 5-monooxygenase activation protein eta, 60S ribosomal protein L18a, CRAL-TRIO domain-containing protein, Peptidase S1 domain-containing protein.

Deiminated proteins identified in EVs only included Desmin, 60 kDa chaperonin, 78 kDa glucose-regulated protein, Septin 7, 160 kDa neurofilament protein, 60S acidic ribosomal protein P0, 60S ribosomal protein L8, 60S ribosomal protein L23, Ribosomal protein L3 like, 75 kDa glucose-regulated protein, OTU deubiquitinase with linear linkage specificity b, FACT complex subunit and Spartin b.

Deiminated proteins identified in whole plasma only included: Activation peptide fragment 1, Angiotensinogen, Serpin peptidase inhibitor (heparin cofactor), Ferritin, Fibrinogen (alpha, beta and gamma-chain), Fibronectin, Fibrinopeptide A, Albumin domain-containing protein, Trypsinogen b2, Adiponectin, TED\_complement domain-containing protein, Tubulin beta chain, L-lactate dehydrogenase, Jacalin-type lectin domain-containing protein, Cytoglobin, M20\_dimer domain-containing protein, Alpha-1,4 glucan phosphorylase, Triosephosphate isomerase, AMP deaminase, Fructose-bisphosphate aldolase, Carnosine dipeptidase 2, Ribosomal protein L7, 60S ribosomal protein L13a, Ribosomal protein L4, Ribosomal protein L23a, 40S ribosomal protein S9 and S11, 60S ribosomal protein L21, 40S ribosomal protein S26, Carbonic anhydrase, 3-hydroxyacyl-[acyl-carrier-protein] dehydratase, H15 domain-containing protein, Erythrocyte membrane protein band 4.1 like 2, Cap methyltransferase 1, Olfactomedin 4, PLAT domain-containing protein, Ankyrin repeat domain 28, Centromere protein S, Kringle domain-containing protein, Glutamine-fructose-6-phosphate transaminase, Palmitoyltransferase, Protein kinase domain-containing protein, KIF-binding protein, DDE\_Tnp\_1\_7 domain-containing protein, LRRNT domain-containing protein, Anoctamin, Vesicle-fusing ATPase and Myosin motor domain-containing protein.

Selected target proteins of deimination from above, common to plasma and EVs, and also ones specific to plasma or EVs respectively, are discussed below in relation to known functions and for putative relevance for deimination to their function throughout phylogeny; including in relation to the lamprey literature where available.

**Histones H2A, H2B, H3 and H4** were identified to be deiminated in both lamprey plasma and plasma-EVs in the current study and these are known deimination targets with roles in epigenetic regulation and anti-pathogenic responses in a range of taxa (Pamenter et al., 2019; Criscitiello et al., 2020b) as well as in relation to gene regulation in human pathologies, including cancer (Lange et al., 2017; Fuhrmann and Thompson, 2016; Beato and Sharma, 2020). Histone H3 deimination, in relation to NETosis, including in a range of taxa, has been discussed above (see also Burgener and Schroder, 2020). Histones can furthermore serve as antimicrobial compounds as reported in human (Lee et al.,

2009) and various other taxa including mollusks (Li et al., 2007; De Zoysa et al., 2009; Seo et al., 2011; Dorrington et al., 2011), crustaceans (Smith and Dyrzynda, 2015; Sruthy et al., 2019), amphibians (Cho et al., 2009), teleosts (Fernandes et al., 2002), reptiles (Kozłowski et al., 2016) and pinnipeds (Villagra-Blanco et al., 2019). In lamprey, histones have been assessed in sperm (Saperas et al., 1997) and histone acetylation has been related to neural regeneration (Chen et al., 2016a), but deimination of histones in lamprey has not been reported before. Histone deimination has, in addition to NETosis and gene regulation, also been related to neural regeneration in avian and murine models (Lange et al., 2011; Lange et al., 2014) as well as neurodegenerative disease (Sancandi et al., 2021). The regulation of multifaceted functions of histones, including via post-translational modifications such as deimination, requires further investigation throughout phylogeny, both in relation to physiological roles, including gene regulation, development and tissue regeneration, as well as anti-pathogenic responses.

**Actin** was a common deimination target in EVs and whole plasma. Actin is the major cytoskeletal protein in cells and actin filaments are important for the transport of secretory vesicles, endosomes and mitochondria (DePina and Langford, 1999), and deimination may add to the multifaceted functions carried out by actins. Indeed, deimination of actin has been identified in a range of taxa, including Crustacea (Bowden et al., 2020b) and Mollusca (Bowden et al., 2020c) and has furthermore been associated with EV biogenesis in mammalian cells (Kholia et al., 2015).

**Elongation factor 1 alpha** was identified as a deimination hit in both plasma and plasma-EVs. It has multiple roles in metabolic function, cell growth, cytoskeleton organisation apoptosis, nuclear export of proteins and the immune response (Khacho et al., 2008; Talapatra et al., 2002, Vera et al., 2014). It has for example been associated with stress tolerance in Mollusca (Zapata et al., 2009; Woo et al., 2011). Previously, it has been identified as a deimination candidate in teleosts (Magnadottir et al., 2018a) and in Crustacea (Bowden et al., 2020b). The roles for deimination in multifaceted functions of elongation factor 1 alpha will need further exploration across taxa.

**Glyceraldehyde-3-phosphate dehydrogenase (GAPDH)** was a common target in EVs and plasma. It is an evolutionarily conserved enzyme (Martin and Cerff, 2017) with key functions in the glycolytic pathway, as well as having roles in DNA repair, membrane fusion, and nuclear RNA export (Baibai et al., 2010; Nicholls et al., 2012). GAPDH has previously been identified as deiminated in teleost fish (Magnadottir et al., 2018a), in Mollusca (Bowden et al., 2020c) and in Crustacea (Bowden et al., 2020b). To what extent deimination contributes to GAPDH function in different taxa remains to be investigated.

**Heat shock protein (HSP) 90** was a common deimination target in both EVs and whole plasma. HSP90 participates amongst other in the protein folding response, cell cycle control, organism development and the proper regulation of cytosolic proteins and cell damage during stress, including thermal stress and bacterial challenge (Liang et al., 2015; Liu et al., 2016; Wood et al., 1998). In lamprey, HSP90 has been assessed as in metamorphosis, both in relation to water temperature (Wood et al., 1998) and to inform postembryonic development, including as a comparative model in relation to human pathologies such as infant biliary atresia (Chung-Davidson et al., 2015). HSP has previously been reported as a deimination candidate in rheumatoid arthritis, facilitating deimination-induced shifts in protein structure which aid B cell tolerance bypassing (Travers et al.,

2016). In other taxa, HSP90 was found deiminated in llama serum under normal physiological conditions (Criscitiello et al., 2020a), as well as in Mollusca (Bowden et al., 2020c). It may therefore be of considerable interest how HSP90 is regulated throughout phylogeny and how deimination may contribute to protein moonlighting functions.

**SERPIN domain containing proteins** were identified to be deiminated in both plasma and plasma-EVs, while serpin peptidase inhibitor was identified as a deimination target in whole plasma. These serine proteinases have multifaceted roles in protease inhibition, chromatin organisation, hormone transport, control of apoptosis, as well as in innate immunity, including in anti-microbial and anti-viral responses (Florin-Christensen et al., 2017; Ragg et al., 2007; Laporte et al., 2017). In lamprey, serpins have been described in lamprey innate immunity, including in relation to bacterial infection and as negative regulators of complement activation via binding to C1q (Wang et al., 2019b). This is the first report on deimination in lamprey serpins, but previous studies have identified serpins as deimination targets in alligator and bovine serum and serum-EVs (Criscitiello et al., 2020b,c). In rheumatoid arthritis, deimination has been related to serpin-mediated pathways (Tilvawala et al., 2018) and therefore the role for deimination in physiological and pathological function of serpins may be of interest.

A range of **ribosomal proteins** was identified as deiminated both in lamprey plasma as well as plasma-EVs. Ribosomal proteins are structural components of the protein synthetic machinery and play important and multifaceted roles in protein synthesis (Gerst, 2018; Baßler and Hurt, 2019). They have furthermore been related to mucosal and innate immune responses and anti-microbial effects (Moon et al., 2011; Nuding et al., 2013; Moon et al., 2014; Seo et al., 2017), as well as oxidative stress (Kournoutou et al., 2017) and in lamprey have also been studied in CNS regeneration (Jin et al., 2016). Ribosomes have been identified as deimination candidate in other taxa, including in human (Guo et al., 2011), teleost (Magnadottir et al., 2018a) and Mollusca (Bowden et al., 2020c). Roles for deimination in regulation of ribosomes may be of considerable interest across phylogeny, both in physiological and pathological context.

**Fibrinogen domain-containing protein** was found to be deiminated in plasma and plasma-EVs. Fibrinogen domain containing molecules have ancestral roles in immunity (Hanington and Zhang, 2010; Adema, 2015; Allam and Raftos, 2015). Furthermore, fibrinogen was found deiminated in plasma and in the lamprey, fibrinogen forms part of the blood coagulation network (Davidson et al., 2003). Fibrinogen has previously been found to be deiminated and related to autoimmune disease in human (Hida et al., 2004; Blachère et al., 2017) and has furthermore been identified as deiminated in a range of other taxa including reptiles, camelid and mollusks (Criscitiello et al., 2020a,b; Bowden et al., 2020c). This is first report of deiminated fibrinogen and fibrinogen domains in lamprey, and such post-translational modification may contribute to various immune and coagulation roles throughout the phylogenetic tree.

**C1q domain containing protein (C1qDC) and C1q-TNF-related protein-9** were identified as deimination candidates in lamprey plasma and plasma-EVs. C1q is part of the complement pathway, but C1q domains are also found in a group of non-complement proteins that can act as pattern recognition molecules in innate immunity (Yu et al., 2008). C1qDCs have been identified in lamprey and related to roles in immunity (Nakamura et al., 2009; Pei et al., 2016), while C1q forms part of the complement system. Lamprey C1q is unusual as it acts as a lectin (Matsushita et al., 2004), activating

C3 in association with MASP via the lectin pathway (Dodds and Matsushita, 2007; Matsushita 2018). Lamprey C1q can furthermore interact with a secreted type of VLR (VLRB) in a complex with antigens, and may via MASP, mediate activation of C3, resulting in cytolysis. The C1q/TNF-related proteins (CTRPs) superfamily is involved in diverse processes including inflammation, apoptosis, host defense, autoimmunity, organogenesis, cell differentiation, insulin resistance and hibernation (Chen et al., 2016b). Several C1Q/TNF related proteins have been identified in river lamprey (*Eudontomyzon morii*) and related to immune response or injury repair processes (Chen et al., 2016b). The deimination of C1q has previously been identified in several taxa, including in mammals (Criscitiello et al., 2020c) and reptiles (Criscitiello et al., 2020b) and C1q domain containing proteins were also identified to be deiminated in Mollusca (Bowden et al., 2020c). How deimination is involved in the multifaceted roles of C1q proteins may be of some interest and may possibly also contribute to various functions taken on throughout vertebrate development. It may be of interest that C1q-TNF-related protein-9 belongs to the adiponectin family and is furthermore known to interact with adiponectin, which in the current study was also identified as a deimination candidate in lamprey whole plasma.

**Adiponectin** was identified as deiminated in lamprey whole plasma. Adiponectin is a secreted adipokine, it acts as a regulator of immune and metabolic functions in mammals and plays key roles in glucose regulation (Fiaschi, 2019). Adiponectin is linked to longevity and regenerative functions, as well as embryonic development (Chen et al., 2019; Fiaschi et al., 2014; Barbe et al., 2019). It has furthermore roles in various pathologies, such as myopathies, cancers and obesity (Gamberi et al., 2019; Parida et al., 2019). In fish (ayu, *Plecoglossus altivelis*) it has been related to immunity, including regulation of monocyte/macrophage function and roles in regulation of anti- and pro-inflammatory cytokines (Liu et al., 2018a). Adiponectin has been studied in lamprey, where it has been found to play roles in immunity, to induce inflammatory cytokine production, inhibit cell proliferation and to promote apoptosis (Zhang et al., 2019). Roles for post-translational modifications in adiponectin have not been much assessed, but adiponectin was recently identified as a deimination candidate in sera and plasma of the following animals with unusual immune and metabolic properties: orca (*Orcinus orca*), llama (*Lama glama*) and the naked mole-rat (*Heterocephalus glaber*) (Magnadottir et al., 2020b; Criscitiello et al., 2019; Pamenter et al., 2019). It may be postulated that post-translational changes, such as deimination, contribute to the multifaceted functions of adiponectin in physiological and pathological processes.

**Myosin motor domain containing protein** and **Ankyrin repeat domain 28** were found to be deiminated in whole plasma. Myosin motors have, like actin, been found to be involved in the cellular transport of secretory vesicles, endosomes and mitochondria (DePina and Langford, 1999) and can furthermore contain ankyrin domains. Ankyrin domains contain beta-turn motifs and are involved in a range of cellular tasks (Devi et al., 2004). ANKRD28 has been associated with regulation of focal adhesion and cell migration (Tachibana et al., 2009) and has been identified to interact with the breast and ovarian cancer-susceptibility gene 1 (BRCA-1) in tumour-suppressor function (Vincent et al., 2016). Ankyrin 28 domains are also found in evolutionary conserved ion channel proteins (Schüler et al., 2015). It may be considered that post-translational deimination can contribute to their various functions.

**Tubulin** (beta chain) was here identified as deiminated in whole plasma. Tubulin has roles in the rearrangement of the cytoskeleton and has been studied in lamprey CNS regeneration (Jin et al.,

2016). Tubulin has been identified as a deimination candidate in llama (Criscitiello et al., 2020a) as well as being, in deiminated form, associated with EV biogenesis and release (Kholia et al., 2015). Deimination of tubulin may be of importance for facilitating EV-mediated processes in homeostasis, immune responses and in relation to various pathologies as well as in cellular communication.

**Ferritin** was identified as deiminated in whole lamprey plasma. Ferritin is the major iron storage protein and central to iron homeostasis, playing roles in physiological processes such as cell proliferation, energy metabolism and nucleic acid synthesis (Moreira et al., 2020), but also in pathological processes (Knovich et al., 2009). In lamprey, ferritin is the plasma iron binding protein (Macey et al., 1982) and the iron regulatory element is highly conserved from lamprey to vertebrates (Andersen et al., 1998). Ferritin is associated with various inflammatory diseases, including cancer, neurodegeneration and infection (Moreira et al., 2020). Furthermore, ferritin regulation can play roles in withholding iron from pathogens and therefore may be important for immunomodulation (McCullough and Bolisetty, 2020). Roles for deimination in the regulation of ferritin may therefore be of considerable importance given also that deimination is associated with a number of pathologies and infectious disease. Ferritin has previously been identified as a deimination candidate in llama serum (Criscitiello et al., 2020a) and its post-translational regulation may play roles in ferritin multifaceted and conserved functions across the phylogeny tree.

**Jacalin**-type lectin domain was a deimination candidate in whole plasma. Jacalin-type lectins are a carbohydrate binding family of lectins that can be galactose or mannose-specific (Peumans et al., 2000). Jacalin type lectins are found across phyla, including archaea (Sivaji et al., 2021). They were first described in plants, where they participate in plant pathogen responses (Esch and Schaffrath, 2017) and plant-derived jacalin has furthermore been reported activate human B cells for immunoglobulin secretion and found to bind IgA (Roque-Barreira and Campos-Neto, 1985). Several jacalin-related lectin proteins have been identified in fish (Cao and Lv, 2016) including in skin mucosa (Rajan et al., 2017). In lamprey, natterin-like proteins with jacalin-like domain containing proteins have been described and shown to have pore-forming and cytotoxic activity and are suggested to act together with VLRs and complement molecules against pathogens and tumour cells (Wu et al., 2017; Chi et al., 2018). Jacalin-like domains are rich in beta sheets, which are structurally susceptible to deimination (Györgi et al., 2006). To what extent deimination contributes to the multifaceted functions of jacalin-like domain containing proteins in immune defences across phylogeny requires further investigation.

**LRRNT** domain-containing protein was deiminated in whole plasma. Leucine rich repeats (LRR) are a highly conserved motif in various physiological functions (Kobe and Kajava, 2001) and form an important structural part of the various immune pattern recognition molecules across phylogeny (Zhang et al., 2020). They are found for example in toll like receptors and C-type lectin receptors of vertebrates (Kang and Lee, 2011; Zhang et al., 2020), while in plants NBS-LRR play part in immune defence (DeYoung and Innes, 2006). LRR domain containing proteins have also been recently described in innate immune responses of shrimp (Zhang et al., 2020). In jawless fish, including lamprey, LRR motives are found in the recombinatorial antigen receptors variable lymphocyte receptors (VLRs) (Pancer et al., 2004). The peptide identified to be deiminated from this protein (RGAFDNLKS) in the current study is an exact match to a common LRRVe-Connecting peptide junction sequence found in about 75% of assembled sea lamprey VLRB proteins. VLRB, found in both lampreys and hagfishes, is expressed in plasma as a multivalent, soluble antigen receptor that

functions analogously to immunoglobulins in jawed vertebrates. Interestingly, both shark novel antigen receptor (NAGR) and llama nanobodies were recently identified to be deimination targets (Criscitello et al., 2019; Criscitello et al., 2020a). It may be postulated that deimination can add to variability in the function of the LRR containing proteins of lamprey, including VLRs.

**Palmitoyltransferase** was a deiminated target protein in whole plasma. Palmitoyltransferase is found as carnitine palmitoyltransferase family, which are mitochondrial enzymes with roles in fatty acid metabolism, including via fatty acid  $\beta$ -oxidation. Palmitoyltransferase is involved in lipid metabolism in neurones and may be involved in demyelinating disease (Davis et al., 2020). Palmitoyltransferase also acts as a regulator of complex-lipid metabolism in cancer metabolism and is implicated in rendering cancer cells resistant to glucose- and oxygen-deprivation (Casals et al., 2016; Qu et al., 2017). Furthermore, it has been linked to mitochondria-associated metabolic reprogramming in the regulation of cancer cell senescence (Wang et al., 2018a). There are also various associations with rare disorders in infants including hypoketotic hypoglycemia, hepatic encephalopathy and seizures (Collins et al., 2010; Wieser et al., 2014). Furthermore palmitoyltransferase is linked to insulin resistance and type II diabetes, with free fatty acid levels elevated and accumulation of fat in skeletal muscle fibres (Rasmussen et al., 2002; Lehmann et al., 2017). In teleost fish, palmitoyltransferase has been associated with cold resistance in relation to lipid catabolism and autophagy during fasting, using zebrafish models (Lu et al., 2019), and in fasting-induced fatty acid oxidation in yellow croaker (Wang et al., 2019c). It has furthermore been assessed in lipid metabolism during obesogenic diet using medaka fish (Torró-Montell et al., 2019), while different isoforms have been identified to have roles in grass carp liver during nutritional limitation (Shi et al., 2017). In elasmobranchs, activities of this fatty acid catabolising enzyme was shown to be 5% the rate of what is seen in teleosts, and in hagfish carnitine palmitoyltransferase rate was 10% compared with teleosts (Moyes et al., 1990). In lamprey, palmitoyltransferase was reported high in liver and muscle, possibly linked to high metabolic activity during sexual maturation (Power et al., 1993), while in larval lamprey relatively low activity has also been reported, which is possibly diet related and to spare from essential fatty acid oxidation (Stonell et al., 1997). It has been furthermore shown that carnitine palmitoyl transferase activities in kidney and rectal gland in elasmobranchs contributes to extrahepatic lipid oxidation (Speers-Roesch et al., 2006). The carnitine palmitoyltransferase family has also been described in Crustacea, showing differences in tissue distribution and variations between genders, indicative of different roles in fatty acid  $\beta$ -oxidation (Liu et al., 2018b). Deimination of palmitoyltransferase is here reported for the first time. Due to important roles of palmitoyltransferases in physiological and pathological function, and variation across phylogeny, deimination of this enzyme family may be of considerable interest.

**Anoctamin** was found as a deiminated protein hit in whole plasma. The anoctamin (Tmem16) family are highly conserved calcium activated chloride channel proteins, some of which act as  $\text{Ca}^{2+}$ -activated lipid scramblases (Falzone et al., 2018; Boccaccio et al., 2019). They have wide tissue expression and multifaceted physiological functions, including regulation of epithelial secretion, neuronal cell excitability, smooth muscle contraction and repair of skeletal muscle membrane (Kunzelmann et al., 2011; Benarroch 2017). Interestingly, anoctamin function in  $\text{Ca}^{2+}$ -dependent phospholipid scrambling has also highlighted their roles in extracellular vesicle release (Whitlock and Hartzell, 2017). Anoctamins have critical roles in many pathologies such as cancer, muscular dystrophy, spinocerebellar ataxia, bleeding disorders and neurological disease (Duran and Hartzell, 2011; Kunzelmann et al., 2011; Benarroch, 2017). In cancers, anoctamins were found to affect

cancer progression, increase cell proliferation, migration and invasion (Xuan et al., 2019; Pinto et al., 2020; Katsurahara et al., 2021). In teleost fish, anoctamin expression is found in enteric neuronal subpopulations (Uyttebroek et al., 2013) and is related to rhythmic contractions of the gastrointestinal tract (Brijs et al., 2016). Furthermore anoctamin was associated with hypoxia and angiogenesis in zebrafish (Delcourt et al., 2015) and roles in the teleost olfactory system have also been identified (Olivares and Schmachtenberg, 2019). While anoctamins have been studied in relation to a number of pathologies, studies on post-translational modifications are scarce if any. This is the first report of deimination of anoctamin to our knowledge and it may therefore be of interest how deimination may affect anoctamin and possibly allow for its protein moonlighting functions.

**Olfactomedin 4 (OLFM4)** was identified as deiminated in whole plasma. Olfactomedin proteins are glycoproteins that were initially identified in the bullfrog (Snyder et al., 1991) and evolutionarily conserved throughout the animal kingdom (Anholt, 2014; Li et al., 2019a). They arose early in evolution and have roles in innate immunity and inflammation (Liu and Rodgers, 2016) as well as in development, including the nervous system, play roles in cell adhesion, intercellular interactions and haematopoiesis (Anholt, 2014; Li et al., 2019a). Olfactomedins are also associated to various pathologies; OLFM4 has been associated to various cancers (Guette et al., 2015; Liu and Rodgers, 2016; Ashizawa et al., 2019; Gao et al., 2019), including as a cancer stem cell marker (van der Flier et al., 2009; Grover et al., 2010) and a tumour suppressor (Li et al., 2019b). OLFM4 is also linked to a range of gastric (including cancer) diseases via anti-inflammation, apoptosis, cell adhesion and proliferation (Wang et al., 2018b). It is also characteristic of intestinal stem cells and plays roles in colon and stomach mucosal immunity (Gersemann et al., 2012). Furthermore, OLFM4 was recently identified as a neutrophil subset marker with possible roles in sepsis heterogeneity (Alder et al., 2017) and in ischemia/reperfusion injury (Levinsky et al., 2019). No studies are published to date on OLFM4 in lamprey to our knowledge, while it has been associated with wound healing in carp (Saleh et al., 2018) and gill response of catfish to bacterial infection (Sun et al., 2012). This is the first report that olfactomedins can be deiminated and such post-translational modification may contribute to its diverse functions in health and disease – possibly also throughout the phylogeny tree.

**Spartin b** was identified as deiminated in plasma-EVs. Spartin is a multifunctional protein with roles in the endoplasmic reticulum, in mitochondrial function and interacts amongst other with ubiquitin and nuclear proteins (Milewska et al., 2009). It plays roles in mitochondrial respiration, metabolism and maintenance, and has been shown to play roles in age-associated ROS production, necrosis and apoptosis (Ring et al., 2017). Spartin has been associated with mitochondrial respiratory chain function and mitochondrial dysfunction in Troyer syndrome, which is a form of hereditary spastic paraplegia (Spiegel et al., 2017), and to neurodevelopmental delay via effects on mitochondrial bioenergetics imbalance (Diquigiovanni et al., 2019). Furthermore spartin is linked to axonal function via the BMP signalling pathway (Tsang et al., 2009). Post-translational modifications have not been assessed in relation to spartin function and its diverse roles may be affected via deimination, which is reported here for the first time in lamprey plasma-EVs.

**Septin 7** was a deimination hit in plasma-EVs only. Septins are a conserved family of cytoskeletal GTPases across phylogeny with roles in cytoskeleton organization, cytokinesis and membrane

dynamics (Neubauer and Zieger, 2017). Septin 7 has been linked to a range of cellular processes including in cell proliferation, mRNA processing, RNA splicing and gene regulation, cytokinesis, reproduction and nervous system function, and is furthermore linked to a range of diseases including neurological and autoimmune diseases as well as cancers (Wang et al., 2018c; Desterke and Gassama-Diagne, 2019). Studies in fish have shown roles in immunity and development. In gilthead sea bream, septins were found upregulated in mucosa in response to chronic cold stress (Sanahuja et al., 2019). In zebrafish, septin 7 was found to be necessary for cardiac function with roles in stabilising actin (Dash et al., 2017). While septins have been reported in EVs before (Xu et al., 2015), their deimination is here reported for the first time in any species to our knowledge. Given the diverse functions of Septin 7, its deimination may be of considerable interest and requires further investigation across taxa.

**Desmin b** was identified as deiminated in EVs only. Desmin is an evolutionarily conserved intermediate filament protein with many arginines in its head domain, which plays roles in filament assembly while the tail domain plays roles in integration of filaments and interactions with organelles and proteins (Bär et al., 2004). Desmin is associated with skeletal muscle and embryogenesis, and may also have important roles in mitochondrial function including distribution, morphology, stabilisation and function (Diokmetzidou et al., 2016; Ahmed et al., 2016; Alam et al., 2020; Smolina et al., 2020). Desmin is linked to a number of skeletal and cardiac myopathies as well as neuromuscular disorders (Goebel and Bornemann, 1993; Palmio and Udd, 2016; Herrmann et al., 2020). Desmin has been identified as a target for deimination in human, predominantly of the head domain (Inagaki et al., 1989). This post-translational modification may therefore contribute to its physiological as well as pathological roles and is furthermore identified here in lamprey, indicative of deimination facilitating desmin function across phylogeny.

In summary, the current study characterised lamprey plasma-EVs for the first time, alongside identifying deimination signatures in EVs as well as whole plasma. Evidence for a PAD-like protein in lamprey plasma was based on cross-reaction with human PAD antibodies, and correlates with that lamprey PAD2-like amino acid sequences have previously been reported for lamprey. Deiminated protein profiles identified here in lamprey plasma and plasma-EVs indicate regulatory mechanisms via post-translational deimination of some major metabolic, immune related and gene regulatory pathways. Our findings show that deiminated protein cargo in plasma-EVs differs compared with whole plasma, and this corresponds to findings from previous comparative studies assessing differences in functional protein pathways for deiminated proteins in whole serum/plasma versus EVs in diverse taxa. Indeed, a vaster range of reactome pathways was here identified to be enriched for deiminated proteins in lamprey plasma-EVs, indicating important roles for EV-mediated cellular communication in health and disease. As current knowledge of deimination mediated regulation of proteins is scarce, future focussed studies on selected key proteins, for example using site directed mutagenesis, will need to be performed to assess changes in protein function and downstream consequences on selected immune, gene regulatory and metabolic network function. Furthermore, assessment of changes in deimination signatures in response to stressors, such as infection and environmental changes, may help identifying roles for deimination in intracellular trafficking and cell communication as well as aiding biomarker discovery. Changes in deimination targets and EV

signatures have indeed been recently identified in teleost fish kept at different environmental temperatures (Magnadottir et al., 2020a).

The identification of deimination regulated pathways in lamprey in the current study provides novel insights into post-translational regulation of conserved and species-specific pathways relating to immunity, metabolism and gene regulation, and can furthermore be related to similar analysis carried out in other taxa across the phylogeny tree.

## 5. Conclusion

The analysis of deiminated proteins in lamprey indicates that protein deimination affects multiple pathways involved in immunity and metabolism, as well as in gene regulation and this has previously been identified both in human disease as well as in diverse taxa, albeit with some species specific differences. Such post-translational regulation therefore may be a hitherto under-recognised conserved control switch of immune and metabolic pathways throughout the phylogenetic tree, placing PADs in an interesting position as a conserved regulator in facilitating multifaceted protein functions via protein moonlighting. This study also contributes to furthering understanding of EV cargos and their roles in intracellular trafficking and cell communication in immune, metabolic and gene regulation across the phylogeny tree.

**Acknowledgements** The authors would like to thank Yagnesh Umrana and Michael Deery at the Cambridge Centre for Proteomics for the LC-MS/MS analysis. The study was funded in part by University of Westminster internal funding to SL. S D'A. is a recipient of a University of Westminster SLS Studentship. JPR is funded by the U.S.A. National Institutes of Health grant R01AI1072435 to Max D. Cooper. Thanks are due to The Guy Foundation for funding the purchase of equipment utilised in this work.

### Author Contributions Statement

**JR:** Resources; Validation; Writing - review & editing.

**IK:** Methodology; Resources; Visualization.

**SA:** Visualisation, Writing-review & editing.

**SL:** Conceptualization; Data curation; Formal analysis; Funding acquisition; Investigation; Methodology; Project administration; Resources; Validation; Visualization; Writing -original draft; Writing - review & editing.

**Conflict of Interest Statement:** JR is a consultant for NovAb, Inc., a biotech company that produces lamprey antibodies for biomedical use. All other authors declare no conflicting interest.

Adema, C.M., 2015. Fibrinogen-Related Proteins (FREPs) in Mollusks. *Results Probl Cell Differ.* 57, 111-29.

Ahmed, M.I., Guichard, J.L., Soorappan, R.N., Ahmad, S., Mariappan, N., Litovsky, S., Gupta, H., Lloyd, S.G., Denney, T.S., Powell, P.C., Aban, I., Collawn, J., Davies, J.E., McGiffin, D.C., Dell'Italia, L.J., 2016. Disruption of desmin-mitochondrial architecture in patients with regurgitant mitral valves and preserved ventricular function. *J Thorac Cardiovasc Surg.* 152(4), 1059-1070.e2.

- Alder, M.N., Rogozin, I.B., Iyer, L.M., Glazko, G.V., Cooper, M.D., Pancer, Z., 2005. Diversity and function of adaptive immune receptors in a jawless vertebrate. *Science*. 310(5756), 1970-3.
- Alder, M.N., Opoka, A.M., Lahni, P., Hildeman, D.A., Wong, H.R., 2017. Olfactomedin-4 Is a Candidate Marker for a Pathogenic Neutrophil Subset in Septic Shock. *Crit Care Med*. 45(4), e426-e432.
- Alghamdi, M., Alasmari, D., Assiri, A., Mattar, E., Aljaddawi, A.A., Alattas, S.G., Redwan, E.M., 2019. An Overview of the Intrinsic Role of Citrullination in Autoimmune Disorders. *J. Immunol. Res*. 2019, 7592851.
- Alam, S., Abdullah, C.S., Aishwarya, R., Morshed, M., Nitu, S.S., Miriyala, S., Panchatcharam, M., Kevil, CG, Orr, A.W., Bhuiyan, M.S., 2020. Dysfunctional Mitochondrial Dynamic and Oxidative Phosphorylation Precedes Cardiac Dysfunction in R120G- $\alpha$ B-Crystallin-Induced Desmin-Related Cardiomyopathy. *J Am Heart Assoc*. 9(23), e017195.
- Andersen, O., Pantopoulos, K., Kao, H.T., Muckenthaler, M., Youson, J.H., Pieribone, V., 1998. Regulation of iron metabolism in the sanguivore lamprey *Lampetra fluviatilis*--molecular cloning of two ferritin subunits and two iron-regulatory proteins (IRP) reveals evolutionary conservation of the iron-regulatory element (IRE)/IRP regulatory system. *Eur J Biochem*. 254(2), 223-9.
- Anholt, R.R., 2014. Olfactomedin proteins: central players in development and disease. *Front Cell Dev Biol*. 2:6.
- Antwi-Baffour, S., Malibha-Pinchbeck, M., Stratton, D., Jorfi, S., Lange, S., Inal, J., 2019. Plasma mEV levels in Ghanain malaria patients with low parasitaemia are higher than those of healthy controls, raising the potential for parasite markers in mEVs as diagnostic targets. *J. Extracell. Vesicles*. 9(1), 1697124.
- Ashizawa, Y., Kuboki, S., Nojima, H., Yoshitomi, H., Furukawa, K., Takayashiki, T., Takano, S., Miyazaki, M., Ohtsuka, M., 2019. OLFM4 Enhances STAT3 Activation and Promotes Tumor Progression by Inhibiting GRIM19 Expression in Human Hepatocellular Carcinoma. *Hepatol Commun*. 3(7), 954-970.
- Baibai, T., Oukhattar, L., Mountassif, D., Assobhei, O., Serrano, A., Soukri, A., 2010. Comparative molecular analysis of evolutionarily distant glyceraldehyde-3-phosphate dehydrogenase from *Sardina pilchardus* and *Octopus vulgaris*. *Acta Biochim Biophys Sin (Shanghai)*. 42(12), 863-72.
- Barbe, A., Bongrani, A., Mellouk, N., Estienne, A., Kurowska, P., Grandhay, J., Elfassy, Y., Levy, R., Rak, A., Froment, P., et al., 2019. Mechanisms of adiponectin action in fertility: An overview from gametogenesis to gestation in humans and animal models in normal and pathological conditions. *Int. J. Mol. Sci*. 20, 1526.
- Bär, H., Strelkov, S.V., Sjöberg, G., Aebi, U., Herrmann, H., 2004. The biology of desmin filaments: how do mutations affect their structure, assembly, and organisation? *J Struct Biol*. 148(2), 137-52.
- Beato, M, Sharma, P., 2020. Peptidyl Arginine Deiminase 2 (PADI2)-Mediated Arginine Citrullination Modulates Transcription in Cancer. *Int J Mol Sci*. 21(4), 1351.
- Benarroch, E.E., 2017. Anoctamins (TMEM16 proteins): Functions and involvement in neurologic disease. *Neurology*. 89(7), 722-729.

- Baßler, J., Hurt, E., 2019. Eukaryotic Ribosome Assembly. *Annu Rev Biochem.* 88,281-306.
- Bicker, K.L., Thompson, P.R., 2013. The protein arginine deiminases: Structure, function, inhibition, and disease. *Biopolymers.* 99 (2), 155-63.
- Bielecka, E., Scavenius, C., Kantyka, T., Jusko, M., Mizgalska, D., Szmigielski, B., Potempa, B., Enghild, J.J., Prossnitz, E.R., Blom, A.M., Potempa, J., 2014. Peptidyl arginine deiminase from *Porphyromonas gingivalis* abolishes anaphylatoxin C5a activity. *J. Biol. Chem.* 289, 32481–32487.
- Blachère, N.E., Parveen, S., Frank, M.O., Dill, B.D., Molina, H., Orange, D.E., 2017. High-Titer Rheumatoid Arthritis Antibodies Preferentially Bind Fibrinogen Citrullinated by Peptidylarginine Deiminase 4. *Arthritis Rheumatol.* 69(5), 986-995.
- Boccaccio, A., Di Zanni, E., Gradogna, A., Scholz-Starke, J., 2019. Lifting the veils on TMEM16E function. *Channels (Austin).* 13(1), 33-35.
- Boehm, T., Hirano, M., Holland, S.J., Das, S., Schorpp, M., Cooper, M.D., 2018. Evolution of Alternative Adaptive Immune Systems in Vertebrates. *Annu Rev Immunol.* 36, 19-42.
- Bowden, T.J., Kraev, I., Lange, S., 2020a. Post-translational protein deimination signatures and extracellular vesicles (EVs) in the Atlantic horseshoe crab (*Limulus polyphemus*). *Dev Comp Immunol.* 110, 103714.
- Bowden, T.J., Kraev, I., Lange, S., 2020b. Extracellular vesicles and post-translational protein deimination signatures in haemolymph of the American lobster (*Homarus americanus*). *Fish Shellfish Immunol.* 106, 79-102.
- Bowden, T.J., Kraev, I., Lange, S., 2020c. Extracellular Vesicles and Post-Translational Protein Deimination Signatures in Mollusca-The Blue Mussel (*Mytilus edulis*), Soft Shell Clam (*Mya arenaria*), Eastern Oyster (*Crassostrea virginica*) and Atlantic Jackknife Clam (*Ensis leei*). *Biology (Basel).* 9(12), 416.
- Brijs, J., Hennig, G.W., Kellermann, A.M., Axelsson, M., Olsson, C., 2017. The presence and role of interstitial cells of Cajal in the proximal intestine of shorthorn sculpin (*Myoxocephalus scorpius*). *J Exp Biol.* 220(Pt 3), 347-357.
- Brinkmann, V., Reichard, U., Goosmann, C., Fauler, B., Uhlemann, Y., Weiss, D.S., Weinrauch, Y., Zychlinsky, A., 2004. Neutrophil extracellular traps kill bacteria. *Science.* 303(5663), 1532-5.
- Burgener, S.S., Schroder, K., 2020. Neutrophil Extracellular Traps in Host Defense. *Cold Spring Harb Perspect Biol.* 12(7), a037028.
- Casals, N., Zammit, V., Herrero, L., Fadó, R., Rodríguez-Rodríguez, R., Serra, D., 2016. Carnitine palmitoyltransferase 1C: From cognition to cancer. *Prog Lipid Res.* 61, 134-48.
- Casanova, V., Sousa, F.H., Shakamuri, P., Svoboda, P., Buch, C., D'Acromont, M., Christophorou, M.A., Pohl, J., Stevens, C., Barlow, P.G., 2020. Citrullination Alters the Antiviral and Immunomodulatory Activities of the Human Cathelicidin LL-37 During Rhinovirus Infection. *Front. Immunol.* 11, 85.
- Chen, J., Laramore, C., Shifman, M.I., 2016a. Differential expression of HDACs and KATs in high and low regeneration capacity neurons during spinal cord regeneration. *Exp Neurol.* 280, 50-9.

- Chen, L., Wu, F., Yuan, S., Feng, B., 2016b. Identification and characteristic of three members of the C1q/TNF-related proteins (CTRP) superfamily in *Eudontomyzon morii*. *Fish Shellfish Immunol.* 59, 233-240.
- Chen, Y.L., Tao, J., Zhao, P.J., Tang, W., Xu, J.P., Zhang, K.Q., Zou, C.G., 2019. Adiponectin receptor PAQR-2 signaling senses low temperature to promote *C. elegans* longevity by regulating autophagy. *Nat Commun.* 10(1), 2602.
- Chi, X., Su, P., Bi, D., Tai, Z., Li, Y., Pang, Y., Li, Q., 2018. Lamprey immune protein-1 (LIP-1) from *Lampetra japonica* induces cell cycle arrest and cell death in HeLa cells. *Fish Shellfish Immunol.* 75, 295-300.
- Cho, J.H., Sung, B.H., Kim, S.C., 2009. Buforins: histone H2A-derived antimicrobial peptides from toad stomach. *Biochim Biophys Acta.* 1788(8), 1564-9.
- Chung-Davidson, Y.W., Yeh, C.Y., Bussy, U., Li, K., Davidson, P.J., Nanlohy, K.G., Brown, C.T., Whyard, S., Li, W., 2015. Hsp90 and hepatobiliary transformation during sea lamprey metamorphosis. *BMC Dev Biol.* 15, 47.
- Claushuis, T.A.M., van der Donk, L.E.H., Luitse, A.L., van Veen, H.A., van der Wel, N.N., van Vught, L.A., Roelofs, J.J.T.H., de Boer, O.J., Lankelma, J.M., Boon, L., de Vos, A.F., van 't Veer, C., van der Poll, T., 2018. Role of peptidylarginine deiminase 4 in neutrophil extracellular trap formation and host defense during *Klebsiella pneumoniae*-induced pneumonia-derived sepsis. *J. Immunol.* 201(4), 1241-1252.
- Colombo, M., Raposo, G., Théry, C., 2014. Biogenesis, secretion, and intercellular interactions of exosomes and other extracellular vesicles. *Annu. Rev. Cell. Dev. Biol.* 30, 255–289
- Collins, S.A., Sinclair, G., McIntosh, S., Bamforth, F., Thompson, R., Sobol, I., Osborne, G., Corriveau, A., Santos, M., Hanley, B., Greenberg, C.R., Vallance, H., Arbour, L., 2010. Carnitine palmitoyltransferase 1A (CPT1A) P479L prevalence in live newborns in Yukon, Northwest Territories, and Nunavut. *Mol Genet Metab.* 101(2-3), 200-4.
- Criscitiello, M.F., Kraev, I., Lange, S., 2019. Deiminated proteins in extracellular vesicles and plasma of nurse shark (*Ginglymostoma cirratum*) - Novel insights into shark immunity. *Fish Shellfish Immunol.* 92, 249-255.
- Criscitiello, M.F., Kraev, I., Lange, S., 2020a. Deiminated proteins in extracellular vesicles and serum of llama (*Lama glama*)-Novel insights into camelid immunity. *Mol. Immunol.* 117, 37-53.
- Criscitiello, M.F., Kraev, I., Petersen L.H., Lange, S., 2020b. Deimination Protein Profiles in *Alligator mississippiensis* Reveal Plasma and Extracellular Vesicle- specific Signatures Relating to Immunity, Metabolic Function and Gene Regulation. *Front Immunol.* 11:651.
- Criscitiello, M.F., Kraev, I., Lange, S., 2020c. Post-Translational Protein Deimination Signatures in Serum and Serum-Extracellular Vesicles of *Bos taurus* Reveal Immune, Anti-Pathogenic, Anti-Viral, Metabolic and Cancer-Related Pathways for Deimination. *Int J Mol Sci.* 21(8),2861.
- D'Alessio, S., Thorgeirsdóttir, S., Kraev, I., Skírnisson, K., Lange, S. Post-Translational Protein Deimination Signatures in Plasma and Plasma EVs of Reindeer (*Rangifer tarandus*). *Biology (Basel).* 10(3), 222.

Dash, S.N., Narumanchi, S., Paavola, J., Perttunen, S., Wang, H., Lakkisto, P., Tikkanen, I., Lehtonen, S., 2017. *Sept7b* is required for the subcellular organization of cardiomyocytes and cardiac function in zebrafish. *Am J Physiol Heart Circ Physiol.* 312(5), H1085-H1095.

Davidson, C.J., Tuddenham, E.G., McVey J.H., 2003. 450 million years of hemostasis. *J Thromb Haemost.* 1(7), 1487-94.

Davis, D.L., Mahawar, U., Pope, V.S., Allegood, J., Sato-Bigbee, C., Wattenberg, B.W., 2020. Dynamics of sphingolipids and the serine palmitoyltransferase complex in rat oligodendrocytes during myelination. *J Lipid Res.* 61(4), 505-522.

Desterke, C., Gassama-Diagne, A., 2019. Protein-protein interaction analysis highlights the role of septins in membrane enclosed lumen and mRNA processing. *Adv Biol Regul.* 73, 100635.

DePina, A.S., Langford, G.M., 1999. Vesicle transport: the role of actin filaments and myosin motors. *Microsc Res Tech.* 47(2), 93-106.

De Zoysa, M., Nikapitiya, C., Whang, I., Lee, J.S., Lee, J., 2009. Abhisin: a potential antimicrobial peptide derived from histone H2A of disk abalone (*Haliotis discus discus*). *Fish Shellfish Immunol.* 27(5), 639-46.

Delcourt, N., Quevedo, C., Nonne, C., Fons, P., O'Brien, D., Loyaux, D., Diez, M., Autelitano, F., Guillemot, J.C., Ferrara, P., Muriana, A., Callol, C., Hérault, J.P., Herbert, J.M., Favre, G., Bono, F., 2015. Targeted identification of sialoglycoproteins in hypoxic endothelial cells and validation in zebrafish reveal roles for proteins in angiogenesis. *J Biol Chem.* 290(6), 3405-17.

Deng, Q., Pan, B., Alam, H.B., Liang, Y., Wu, Z., Liu, B., Mor-Vaknin, N., Duan, X., Williams, A.M., Tian, Y., Zhang, J., Li, Y., 2020. Citrullinated Histone H3 as a Therapeutic Target for Endotoxic Shock in Mice. *Front Immunol.* 10, 2957.

Devi, V.S., Binz, H.K., Stumpp, M.T., Plückthun, A., Bosshard, H.R., Jelesarov, I., 2004. Folding of a designed simple ankyrin repeat protein. *Protein Sci.* 13(11), 2864-70.

DeYoung, B.J., Innes, R.W., 2006. Plant NBS-LRR proteins in pathogen sensing and host defense. *Nat Immunol.* 7(12), 1243-9.

Diquigiovanni, C., Bergamini, C., Diaz, R., Liparulo, I., Bianco, F., Masin, L., Baldassarro, V. A., Rizzardi, N., Tranchina, A., Buscherini, F., Wischmeijer, A., Pippucci, T., Scarano, E., Cordelli, D. M., Fato, R., Seri, M., Paracchini, S., Bonora, E., 2019. A novel mutation in *SPART* gene causes a severe neurodevelopmental delay due to mitochondrial dysfunction with complex I impairments and altered pyruvate metabolism. *FASEB J.* 33(10), 11284-11302.

Diokmetzidou, A., Soumaka, E., Kloukina, I., Tsikitis, M., Makridakis, M., Varela, A., Davos, C.H., Georgopoulos, S., Anesti, V., Vlahou, A., Capetanaki, Y., 2016. Desmin and  $\alpha$ B-crystallin interplay in the maintenance of mitochondrial homeostasis and cardiomyocyte survival. *J Cell Sci.* 129(20), 3705-3720.

Dodds, A.W., Matsushita, M., 2007. The phylogeny of the complement system and the origins of the classical pathway. *Immunobiology.* 212(4-5), 233-43.

- Dorrington, T., Villamil, L., Gómez-chiarri, M., 2011. Upregulation in response to infection and antibacterial activity of oyster histone H4. *Fish Shellfish Immunol.* 30(1), 94-101.
- Duran, C., Hartzell, H.C., 2011. Physiological roles and diseases of Tmem16/Anoctamin proteins: are they all chloride channels? *Acta Pharmacol Sin.* 32(6), 685-92.
- El-Sayed, A.S.A., Shindia, A.A., AbouZaid, A.A., Yassin, A.M., Ali, G.S., Sitohy, M.Z., 2019. Biochemical characterization of peptidylarginine deiminase-like orthologs from thermotolerant *Emericella dentata* and *Aspergillus nidulans*. *Enzyme Microb. Technol.* 124, 41-53.
- Falzone, M.E., Malvezzi, M., Lee, B.C., Accardi, A., 2018. Known structures and unknown mechanisms of TMEM16 scramblases and channels. *J Gen Physiol.* 150(7), 933-947.
- Fernandes, J.M., Kemp, G.D., Molle, M.G., Smith, V.J., 2002. Anti-microbial properties of histone H2A from skin secretions of rainbow trout, *Oncorhynchus mykiss*. *Biochem J.* 368(Pt 2), 611-20.
- Fernández-Reiriz, M.J., Navarro, J.M., Labarta, U., 2005. Enzymatic and feeding behaviour of *Argopecten purpuratus* under variation in salinity and food supply. *Comp Biochem Physiol A Mol Integr Physiol.* 141(2), 153-63.
- Fiaschi, T., 2019. Mechanisms of Adiponectin Action. *Int J Mol Sci.* 20(12), pii, E2894.
- Fiaschi, T., Magherini, F., Gamberi, T., Modesti, P.A., Modesti, A., 2014. Adiponectin as a tissue regenerating hormone: More than a metabolic function. *Cell. Mol. Life Sci.*, 71, 1917–1925.
- Florin-Christensen, M., Schnittger, L., Dominguez, M., Mesplet, M., Rodríguez, A., Ferreri, L., Asenzo, G., Wilkowsky, S., Farber, M.; Echaide, I., Suarez, C., 2007. Search for *Babesia bovis* vaccine candidates. *Parassitologia* 49 (Suppl. 1), 9–12.
- Fuhrmann, J., Thompson, P.R., 2016. Protein Arginine Methylation and Citrullination in Epigenetic Regulation. *ACS Chem Biol.* 11(3), 654-68.
- Gamberi, T., Magherini, F., Fiaschi, T., 2019. Adiponectin in myopathies. *Int. J. Mol. Sci.* 20, 1544.
- Gao, X.Z., Wang, G.N., Zhao, W.G., Han, J., Diao, C.Y., Wang, X.H., Li, S.L., Li, W.C., 2019. Blocking OLFM4/HIF-1 $\alpha$  axis alleviates hypoxia-induced invasion, epithelial-mesenchymal transition, and chemotherapy resistance in non-small-cell lung cancer. *J Cell Physiol.* 2019 Jan 24. doi: 10.1002/jcp.28144.
- Gavinho, B., Sabatke, B., Feijoli, V., Rossi, I.V., da Silva, J.M., Evans-Osses, I., Palmisano, G., Lange, S., Ramirez, M.I., 2020. Peptidylarginine Deiminase Inhibition Abolishes the Production of Large Extracellular Vesicles From *Giardia intestinalis*, Affecting Host-Pathogen Interactions by Hindering Adhesion to Host Cells. *Front Cell Infect Microbiol.* 10, 417.
- Gersemann, M., Becker, S., Nuding, S., Antoni, L., Ott, G., Fritz, P., Oue, N., Yasui, W., Wehkamp, J., Stange, E.F., 2012. Olfactomedin-4 is a glycoprotein secreted into mucus in active IBD. *J Crohns Colitis.* 6(4), 425-34.
- Gerst, J.E., 2018. Pimp My Ribosome: Ribosomal Protein Paralogs Specify Translational Control. *Trends Genet.* 34(11), 832-845.

Goebel, H.H., Bornemann, A., 1993. Desmin pathology in neuromuscular diseases. *Virchows Arch B Cell Pathol Incl Mol Pathol.* 64(3), 127-35.

Grover, P.K., Hardingham, J.E., Cummins, A.G., 2010. Stem cell marker olfactomedin 4: critical appraisal of its characteristics and role in tumorigenesis. *Cancer Metastasis Rev.* 29(4), 761-75.

Guette, C., Valo, I., Vétillard, A., Coqueret, O., 2015. Olfactomedin-4 is a candidate biomarker of solid gastric, colorectal, pancreatic, head and neck, and prostate cancers. *Proteomics Clin Appl.* 9(1-2), 58-63.

Guo, P., Hirano, M., Herrin, B.R., Li, J., Yu, C., Sadlonova, A., Cooper, M.D., 2009. Dual nature of the adaptive immune system in lampreys. *Nature.* 459(7248), 796-801. Erratum in: *Nature.* 2009 460(7258):1044.

Guo, Q., Bedford, M.T., Fast, W., 2011. Discovery of peptidylarginine deiminase-4 substrates by protein array: antagonistic citrullination and methylation of human ribosomal protein S2. *Mol Biosyst.* 7(7), 2286-95.

György, B., Toth, E., Tarcsa, E., Falus, A., Buzas, E.I., 2006. Citrullination: a posttranslational modification in health and disease. *Int. J. Biochem. Cell. Biol.* 38, 1662-77.

Hanington, P.C., Zhang, S.M., 2011. The primary role of fibrinogen-related proteins in invertebrates is defense, not coagulation. *J Innate Immun.* 3(1), 17-27.

Henderson, B., Martin, A.C., 2014. Protein moonlighting: a new factor in biology and medicine. *Biochem. Soc. Trans.* 42(6), 1671-8.

Herrmann, H., Cabet, E., Chevalier, N. R., Moosmann, J., Schultheis, D., Haas, J., Schowalter, M., Berwanger, C., Weyerer, V., Agaimy, A., Meder, B., Müller, O. J., Katus, H. A., Schlötzer-Schrehardt, U., Vicart, P., Ferreira, A., Dittrich, S., Clemen, C. S., Lilienbaum, A., & Schröder, R., 2020. Dual Functional States of R406W-Desmin Assembly Complexes Cause Cardiomyopathy With Severe Intercalated Disc Derangement in Humans and in Knock-In Mice. *Circulation.* 142(22), 2155-2171.

Hessvik, N.P., Llorente, A., 2018. Current knowledge on exosome biogenesis and release. *Cell. Mol. Life Sci.* 75 (2), 193-208.

Hida, S., Miura, N.N., Adachi, Y., Ohno, N., 2004. Influence of arginine deimination on antigenicity of fibrinogen. *J Autoimmun.* 23(2), 141-50.

Hirano, M., Guo, P., McCurley, N., Schorpp, M., Das, S., Boehm, T., Cooper, M.D., 2013. Evolutionary implications of a third lymphocyte lineage in lampreys. *Nature.* 501(7467), 435-8.

Inagaki, M., Takahara, H., Nishi, Y., Sugawara, K., Sato, C., 1989. Ca<sup>2+</sup>-dependent deimination-induced disassembly of intermediate filaments involves specific modification of the amino-terminal head domain. *J Biol Chem.* 264(30), 18119-27.

Inal, J.M., Ansa-Addo, E.A., Lange, S., 2013. Interplay of host-pathogen microvesicles and their role in infectious disease. *Biochem. Soc. Trans.* 41 (1), 258-62.

Jeffrey, C.J., 2018. Protein moonlighting: what is it, and why is it important? *Philos. Trans. R. Soc. Lond. B. Biol. Sci.* 373 (1738), pii 20160523.

- Jin, L.Q., Pennise, C.R., Rodemer, W., Jahn, K.S., Selzer, M.E., 2016. Protein synthetic machinery and mRNA in regenerating tips of spinal cord axons in lamprey. *J Comp Neurol.* 524(17), 3614-3640.
- Kang, J.Y., Lee, J.O., 2011. Structural biology of the Toll-like receptor family. *Annu Rev Biochem.* 80, 917-41.
- Katsurahara, K., Shiozaki, A., Kosuga, T., Shimizu, H., Kudou, M., Arita, T., Konishi, H., Komatsu, S., Kubota, T., Fujiwara, H., Okamoto, K., Kishimoto, M., Konishi, E., Otsuji, E., 2021. ANO9 regulates PD-L2 expression and binding ability to PD-1 in gastric cancer. *Cancer Sci.* 112(3), 1026-1037.
- Kholia, S., Jorfi, S., Thompson, P.R., Causey, C.P., Nicholas, A.P., Inal, J.M., Lange, S., 2015. A novel role for peptidylarginine deiminases (PADs) in microvesicle release: A therapeutic potential for PAD inhibitors to sensitize prostate cancer cells to chemotherapy. *J. Extracell. Vesicles.* 4, 26192.
- Knovich, M.A., Storey, J.A., Coffman, L.G., Torti, S.V., Torti, F.M., 2008. Ferritin for the clinician. *Blood Rev.* 23(3), 95-104.
- Kobe, B., Kajava, A.V., 2001. The leucine-rich repeat as a protein recognition motif. *Curr Opin Struct Biol.* 11(6), 725-32.
- Konig, M.F., Andrade, F. A., 2016. Critical Reappraisal of Neutrophil Extracellular Traps and NETosis Mimics Based on Differential Requirements for Protein Citrullination. *Front Immunol.* 7, 461.
- Kournoutou, G.G., Giannopoulou, P.C., Sazakli, E., Leotsinidis, M., Kalpaxis, D.L., 2017. Oxidative damage of 18S and 5S ribosomal RNA in digestive gland of mussels exposed to trace metals. *Aquat Toxicol.* 192, 136-147.
- Kosgodage, U.S., Trindade, R.P., Thompson, P.T., Inal, J.M., Lange, S., 2017. Chloramidine/Bisindolylmaleimide-I-mediated inhibition of exosome and microvesicle release and enhanced efficacy of cancer chemotherapy. *Int J Mol Sci.* 18(5), pii E1007.
- Kosgodage, U.S., Uysal-Onganer, P., Maclatchy, A., Nicholas, A.P., Inal, J.M., Lange, S., 2018. Peptidylarginine deiminases post-translationally deiminate prohibitin and modulate extracellular vesicle release and miRNAs 21 and 126 in glioblastoma multiforme. *Int. J. Mol. Sci.* 20(1), pii E103.
- Kosgodage, U.S., Matewele, P., Mastroianni, G., Kraev, I., Brotherton, D., Awamaria, B., Nicholas, A.P., Lange, S., Inal, J.M., 2019. Peptidylarginine Deiminase Inhibitors Reduce Bacterial Membrane Vesicle Release and Sensitize Bacteria to Antibiotic Treatment. *Front. Cell. Infect. Microbiol.* 9, 227.
- Kozlowski, H.N., Lai, E.T., Havugimana, P.C., White, C., Emili, A., Sakac, D., Binnington, B., Neschadim, A., McCarthy, S.D., Branch, D.R., 2016. Extracellular histones identified in crocodile blood inhibit in-vitro HIV-1 infection. *AIDS.* 30(13), 2043-52.
- Kristmundsson, Á., Erlingsdóttir, Á., Lange, S., 2021. Peptidylarginine Deiminase (PAD) and Post-Translational Protein Deimination-Novel Insights into Alveolata Metabolism, Epigenetic Regulation and Host-Pathogen Interactions. *Biology (Basel).* 10(3), 177.
- Kuraku, S., Kuratani, S., 2006. Time scale for cyclostome evolution inferred with a phylogenetic diagnosis of hagfish and lamprey cDNA sequences. *Zoolog Sci.* 23(12), 1053-64.

Kunzelmann, K., Tian, Y., Martins, J.R., Faria, D., Kongsuphol, P., Ousingsawat, J., Thevenod, F., Roussa, E., Rock, J., Schreiber, R., 2011. Anoctamins. *Pflugers Arch.* 462(2), 195-208.

Lange, S., Gögel, S., Leung, K.Y., Vernay, B., Nicholas, A.P., Causey, C.P., Thompson, P.R., Greene, N.D., Ferretti, P., 2011. Protein deiminases: new players in the developmentally regulated loss of neural regenerative ability. *Dev. Biol.* 355(2), 205-14.

Lange, S., Rocha-Ferreira, E., Thei, L., Mawjee, P., Bennett, K., Thompson, P.R., Subramanian, V., Nicholas, A.P., Peebles, D., Hristova, M., Raivich, G., 2014. Peptidylarginine deiminases: novel drug targets for prevention of neuronal damage following hypoxic ischemic insult (HI) in neonates. *J. Neurochem.* 130 (4), 555-62.

Lange, S., Gallagher, M., Kholia, S., Kosgodage, U.S., Hristova, M., Hardy, J., Inal, J.M., 2017. Peptidylarginine deiminases-roles in cancer and neurodegeneration and possible avenues for therapeutic intervention via modulation of exosome and microvesicle (EMV) release? *Int. J. Mol. Sci.* 18(6), pii E1196.

Lange, S., Kraev, I., Magnadóttir, B., Dodds, A.W., 2019. Complement component C4-like protein in Atlantic cod (*Gadus morhua* L.) - Detection in ontogeny and identification of post-translational deimination in serum and extracellular vesicles. *Dev. Comp. Immunol.* 101, 103437.

Laporte, M., Naesens, L., 2017. Airway proteases: An emerging drug target for influenza and other respiratory virus infections. *Curr. Opin. Virol.*, 24, 16–24.

Lee, D.Y., Huang, C.M., Nakatsuji, T., Thiboutot, D., Kang, S.A., Monestier, M., Gallo, R.L., 2009. Histone H4 is a major component of the antimicrobial action of human sebocytes. *J Invest Dermatol.* 129(10), 2489-96.

Lehmann, D., Motlagh, L., Robaa, D., Zierz, S., 2017. Muscle Carnitine Palmitoyltransferase II Deficiency: A Review of Enzymatic Controversy and Clinical Features. *Int J Mol Sci.* 18(1), 82.

Levinsky, N.C., Mallela, J., Opoka, A.M., Harmon, K., Lewis, H.V., Zingarelli, B., Wong, H.R., Alder, M.N., 2019. The olfactomedin-4 positive neutrophil has a role in murine intestinal ischemia/reperfusion injury. *FASEB J.* 33(12), 13660-13668.

Li, C., Song, L., Zhao, J., Zhu, L., Zou, H., Zhang, H., Wang, H., Cai, Z., 2007. Preliminary study on a potential antibacterial peptide derived from histone H2A in hemocytes of scallop *Chlamys farreri*. *Fish Shellfish Immunol.* 22(6), 663-72.

Li, Q., Liu, A., Gu, X., Su, Z., 2019a. Olfactomedin domain-containing proteins: evolution, functional divergence, expression patterns and damaging SNPs. *Mol Genet Genomics.* 294(4), 875-885.

Li, J., Liu, C., Li, D., Wan, M., Zhang, H., Zheng, X., Jie, X., Zhang, P., Li, J., Hou, H., Sun, Q., 2019b. OLFM4 Inhibits Epithelial-Mesenchymal Transition and Metastatic Potential of Cervical Cancer Cells. *Oncol Res.* 27(7), 763-771.

Liang, H.Y., Wang, Z.X., Lei, Q.N., Huang, R.L., Deng, Y.W., Wang, Q.H., Jiao, Y., Du, X.D., 2015. Molecular cloning and expression analysis of a pearl oyster (*Pinctada martensii*) heat shock protein 90 (HSP90). *Genet Mol Res.* 14(4), 18778-91.

Liu, H., Wu, J., Xu, M., He, J., 2016. A novel biomarker for marine environmental pollution of HSP90 from *Mytilus coruscus*. *Mar Pollut Bull.* 111(1-2), 428-434.

- Liu, W, Rodgers, GP., 2016. Olfactomedin 4 expression and functions in innate immunity, inflammation, and cancer. *Cancer Metastasis Rev.* 35(2), 201-12.
- Liu, H., Lu, X.J., Chen, J., 2018a. Full-length and a smaller globular fragment of adiponectin have opposite roles in regulating monocyte/macrophage functions in ayu, *Plecoglossus altivelis*. *Fish Shellfish Immunol.* 82, 319-329.
- Liu, L., Long, X., Deng, D., Cheng, Y., Wu, X., 2018b. Molecular characterization and tissue distribution of carnitine palmitoyltransferases in Chinese mitten crab *Eriocheir sinensis* and the effect of dietary fish oil replacement on their expression in the hepatopancreas. *PLoS One.* 13(8), e0201324.
- Lu, D.L., Ma, Q., Wang, J., Li, L.Y., Han, S.L., Limbu, S.M., Li, D.L., Chen, L.Q., Zhang, M.L., Du, Z.Y., 2019. Fasting enhances cold resistance in fish through stimulating lipid catabolism and autophagy. *J Physiol.* 597(6), 1585-1603.
- Macey, D.J., Webb, J., Potter, I.C., 1982. Iron levels and major iron binding proteins in the plasma of ammocoetes and adults of the southern hemisphere lamprey *Geotria australis* Gray. *Comp Biochem Physiol A Comp Physiol.* 72(2), 307-12.
- McCullough, K., Bolisetty, S., 2020. Iron Homeostasis and Ferritin in Sepsis-Associated Kidney Injury. *Nephron.* 144(12), 616-620.
- Magnadottir, B., Hayes, P., Hristova, M., Bragason, B.T., Nicholas, A.P., Dodds, A.W., Guðmundsdóttir, S., Lange, S., 2018a. Post-translational protein deimination in cod (*Gadus morhua* L.) ontogeny – novel roles in tissue remodelling and mucosal immune defences? *Dev. Comp. Immunol.* 87, 157-170.
- Magnadottir, B., Hayes, P., Gísladóttir, B., Bragason, B.P., Hristova, M., Nicholas, A.P., Guðmundsdóttir, S., Lange, S., 2018b. Pentraxins CRP-I and CRP-II are post-translationally deiminated and differ in tissue specificity in cod (*Gadus morhua* L.) ontogeny. *Dev. Comp. Immunol.* 87, 1-11.
- Magnadottir, B., Bragason, B.T., Bricknell, I.R., Bowden, T., Nicholas, A.P., Hristova, M., Guðmundsdóttir, S., Dodds, A.W., Lange, S., 2019a. Peptidylarginine deiminase and deiminated proteins are detected throughout early halibut ontogeny - complement components C3 and C4 are post-translationally deiminated in halibut (*Hippoglossus hippoglossus* L.). *Dev. Comp. Immunol.* 92, 1-19.
- Magnadottir, B., Kraev, I., Guðmundsdóttir, S., Dodds, A.W., Lange, S., 2019b. Extracellular vesicles from cod (*Gadus morhua* L.) mucus contain innate immune factors and deiminated protein cargo. *Dev. Comp. Immunol.* 99, 103397.
- Magnadottir, B., Uysal-Onganer, P., Kraev, I., Dodds, A.W., Gudmundsdottir, S., Lange, S., 2020a. Extracellular vesicles, deiminated protein cargo and microRNAs are novel serum biomarkers for environmental rearing temperature in Atlantic cod (*Gadus morhua* L.). *Aquaculture Rep.* 16, 100245.
- Magnadottir, B., Uysal-Onganer, P., Kraev, I., Svansson, V., Hayes, P., Lange, S., 2020b. Deiminated proteins and extracellular vesicles - novel serum biomarkers in whales and orca. *Comp. Biochem. Physiol. Part D Genomics Proteomics.* 34, 100676.

Magnadottir, B., Uysal-Onganer, P., Kraev, I., Svansson, V., Skirnisson, K., Lange, S., 2020c. Deiminated proteins and extracellular vesicles as novel biomarkers in pinnipeds: Grey seal (*Halichoerus grypus*) and harbour seal (*Phoca vitulina*). *Biochimie*. 171-172, 79-90.

Magnadottir B, Kraev I, Dodds AW, Lange S., 2021. The Proteome and Citrullinome of *Hippoglossus hippoglossus* Extracellular Vesicles—Novel Insights into Roles of the Serum Secretome in Immune, Gene Regulatory and Metabolic Pathways. *Int J Mol Sci*. 2021 Jan 16;22(2):875.

Martin, W.F., Cerff, R., 2017. Physiology, phylogeny, early evolution, and GAPDH. *Protoplasma*. 254(5), 1823-1834.

Matsushita, M., Matsushita, A., Endo, Y., Nakata, M., Kojima, N., Mizuochi, T., Fujita, T., 2004. Origin of the classical complement pathway: Lamprey orthologue of mammalian C1q acts as a lectin. *Proc Natl Acad Sci U S A*. 101(27), 10127-31.

Matsushita, M., 2018. The Complement System of Agnathans. *Front Immunol*. 9, 1405.

Milewska, M., McRedmond, J., Byrne, P.C., 2009 Identification of novel spartin-interactors shows spartin is a multifunctional protein. *J Neurochem*. 111(4), 1022-30.

Mondal, S., Thompson, P.R., 2019. Protein arginine deiminases (PADs): Biochemistry and chemical biology of protein citrullination. *Acc. Chem. Res*. 52 (3), 818-832.

Moreira, A.C., Mesquita, G., Gomes, M.S., 2020. Ferritin: An Inflammatory Player Keeping Iron at the Core of Pathogen-Host Interactions. *Microorganisms*. 8(4), 589.

Moyes, C.D., Buck, L.T., Hochachka, P.W., 1990. Mitochondrial and peroxisomal fatty acid oxidation in elasmobranchs. *Am J Physiol*. 258(3 Pt 2), R756-62.

Muraro, S.P., De Souza, G.F., Gallo, S.W., Da Silva, B.K., De Oliveira, S.D., Vinolo, M.A.R., Saraiva, E.M., Porto, B.N., 2018. Respiratory Syncytial Virus induces the classical ROS-dependent NETosis through PAD-4 and necroptosis pathways activation. *Sci. Rep*. 8 (1), 14166.

Nakamura, O., Wada, Y., Namai, F., Saito, E., Araki, K., Yamamoto, A., Tsutsui, S., 2009. A novel C1q family member with fucose-binding activity from surfperch, *Neoditrema ransonnetii* (Perciformes, Embiotocidae). *Fish Shellfish Immunol*. 27(6), 714-20.

Nicholas, A.P., Whitaker, J.N., 2002. Preparation of a monoclonal antibody to citrullinated epitopes: its characterization and some applications to immunohistochemistry in human brain. *Glia*. 37(4), 328-36.

Nicholls, C., Li, H., Liu, J.P., 2012. GAPDH: a common enzyme with uncommon functions. *Clin. Exp. Pharmacol. Physiol*. 39(8), 674-9.

Nuding, S., Antoni, L., Stange, E.F., 2013. The host and the flora. *Dig. Dis*. 31(3-4), 286-92.

Olivares, J., Schmachtenberg, O., 2019. An update on anatomy and function of the teleost olfactory system. *PeerJ*. 7, e7808.

Palić, D., Ostojić, J., Andreasen, C.B., Roth, J.A., 2007. Fish cast NETs: neutrophil extracellular traps are released from fish neutrophils. *Dev Comp Immunol*. 31(8), 805-16.

- Palmio, J., Udd, B., 2016. Myofibrillar and distal myopathies. *Rev Neurol (Paris)*. 172(10), 587-593.
- Pamenter, M.E., Uysal-Onganer, P., Huynh, K.W., Kraev, I., Lange, S., 2019. Post-translational deimination of immunological and metabolic protein markers in plasma and extracellular vesicles of naked mole-Rat (*Heterocephalus glaber*). *Int. J. Mol. Sci.* 20 (21), pii E5378
- Moon Y., 2011. Mucosal injuries due to ribosome-inactivating stress and the compensatory responses of the intestinal epithelial barrier. *Toxins (Basel)*. 3(10), 1263-77.
- Moon Y., 2014. Ribosomal alteration-derived signals for cytokine induction in mucosal and systemic inflammation: noncanonical pathways by ribosomal inactivation. *Mediators Inflamm.* 2014, 708193.
- Novák, L., Zubáčová, Z., Karnkowska, A., Kolisko, M., Hroudová, M., Stairs, C. W., Simpson, A. G., Keeling, P. J., Roger, A. J., Čepička, I., & Hampl, V., 2016. Arginine deiminase pathway enzymes: evolutionary history in metamonads and other eukaryotes. *BMC Evol Biol.* 16(1),197.
- Pancer, Z., Amemiya, C.T., Ehrhardt, G.R., Ceitlin, J., Gartland, G.L., Cooper, M.D., 2004. Somatic diversification of variable lymphocyte receptors in the agnathan sea lamprey. *Nature*. 430(6996):174-80.
- Parida, S., Siddharth, S., Sharma, D., 2019. Adiponectin, obesity, and cancer: Clash of the bigwigs in health and disease. *Int. J. Mol. Sci.* 20, 2519.
- Pei, G., Liu, G., Pan, X., Pang, Y., Li, Q., 2016. L-C1qDC-1, a novel C1q domain-containing protein from *Lethenteron camtschaticum* that is involved in the immune response. *Dev Comp Immunol.* 54(1), 66-74.
- Peumans, W.J., Hause, B., Van Damme, E.J., 2000. The galactose-binding and mannose-binding jacalin-related lectins are located in different sub-cellular compartments. *FEBS Lett.* 477(3), 186-92.
- Phillips, R.A., Kraev, I., Lange, S., 2020. Protein deimination and extracellular vesicle profiles in Antarctic seabirds. *Biology (Basel)*. 9 (1), pii: E15.
- Pinto, M.C., Schreiber, R., Lérias, J., Ousingsawat, J., Duarte, A., Amaral, M., Kunzelmann, K., 2020. Regulation of TMEM16A by CK2 and Its Role in Cellular Proliferation. *Cells.* 9(5), 1138.
- Qu, Q., Zeng, F., Liu, X., Wang, Q.J., Deng, F., 2016. Fatty acid oxidation and carnitine palmitoyltransferase I: emerging therapeutic targets in cancer. *Cell Death Dis.* 7(5), e2226.
- Ragg, H., 2007. The role of serpins in the surveillance of the secretory pathway. *Cell. Mol. Life Sci.* 64, 2763–2770.
- Rajan, B., Patel, D.M., Kitani, Y., Viswanath, K., Brinchmann, M.F., 2017. Novel mannose binding natterin-like protein in the skin mucus of Atlantic cod (*Gadus morhua*). *Fish Shellfish Immunol.* 68, 452-457.
- Ramirez, S.H., Andrews, A.M., Paul, D., Pachter, J.S., 2018. Extracellular vesicles: mediators and biomarkers of pathology along CNS barriers. *Fluids Barriers CNS.* 15(1), 19.

Rebl, A, Köllner, B, Anders, E, Wimmers, K, Goldammer, T., 2010. Peptidylarginine deiminase gene is differentially expressed in freshwater and brackish water rainbow trout. *Mol. Biol. Rep.* 37 (5), 2333-9.

Ring, J., Rockenfeller, P., Abraham, C., Tadic, J., Poglitsch, M., Schimmel, K., Westermayer, J., Schauer, S., Achleitner, B., Schimpel, C., Moitzi, B., Rechberger, G. N., Sigrist, S. J., Carmona-Gutierrez, D., Kroemer, G., Büttner, S., Eisenberg, T., Madeo, F., 2017. Mitochondrial energy metabolism is required for lifespan extension by the spastic paraplegia-associated protein spartin. *Microb Cell.* 4(12), 411-422.

Roque-Barreira, M.C., Campos-Neto, A., 1985. Jacalin: an IgA-binding lectin. *J Immunol.* 134(3), 1740-3. PMID: 3871459.

Saleh, M., Kumar, G., Abdel-Baki, A.A., Dkhil, M.A., El-Matbouli, M., Al-Quraishy, S., 2018. Quantitative shotgun proteomics distinguishes wound-healing biomarker signatures in common carp skin mucus in response to *Ichthyophthirius multifiliis*. *Vet Res.* 49(1), 37.

Sanahuja, I., Fernández-Alacid, L., Sánchez-Nuño, S., Ordóñez-Grande, B., Ibarz, A., 2019. Chronic Cold Stress Alters the Skin Mucus Interactome in a Temperate Fish Model. *Front Physiol.* 9, 1916.

Sancandi, M., Uysal-Onganer, P., Kraev, I., Mercer, A., Lange, S., 2021. Protein Deimination Signatures in Plasma and Plasma-EVs and Protein Deimination in the Brain Vasculature in a Rat Model of Pre-Motor Parkinson's Disease. *Int J Mol Sci.* 21(8), 2743.

Saperas, N., Chiva, M., Ribes, E., Kasinsky, H.E., Rosenberg, E., Youson, J.H., Ausio, J., 1994. Chromosomal Proteins of the Sperm of a Cephalochordate (*Branchiostoma floridae*) and an Agnathan (*Petromyzon marinus*): Compositional Variability of the Nuclear Sperm Proteins of Deuterostomes. *Biol Bull.* 186(1), 101-114.

Schüler, A., Schmitz, G., Reft, A., Özbek, S., Thurm, U., Bornberg-Bauer, E., 2015. The Rise and Fall of TRP-N, an Ancient Family of Mechanogated Ion Channels, in Metazoa. *Genome Biol Evol.* 7(6), 1713-27.

Seo, J.K., Stephenson, J., Noga, E.J., 2011. Multiple antibacterial histone H2B proteins are expressed in tissues of American oyster. *Comp Biochem Physiol B Biochem Mol Biol.* 158(3), 223-9.

Seo, J.K., Kim, D.G., Oh, R., Park, K.S., Lee, I.A., Cho, S.M., Lee, K.Y., Nam, B.H., 2017. Antimicrobial effect of the 60S ribosomal protein L29 (cgRPL29), purified from the gill of pacific oyster, *Crassostrea gigas*. *Fish Shellfish Immunol.* 2017 Aug;67:675-683.

Shi, X.C., Sun, J., Yang, Z., Li, X.X., Ji, H., Li, Y., Chang, Z.G., Du, Z.Y., Chen, L.Q., 2017. Molecular characterization and nutritional regulation of carnitine palmitoyltransferase (CPT) family in grass carp (*Ctenopharyngodon idellus*). *Comp Biochem Physiol B Biochem Mol Biol.* 203, 11-19.

Sivaji, N., Suguna, K., Surolia, A., Vijayan, M., 2021. Structural and related studies on Mevo lectin from *Methanococcus voltae* A3: the first thorough characterization of an archeal lectin and its interactions. *Glycobiology.* 31(3), 315-328.

Smith, J. J., Kuraku, S., Holt, C., Sauka-Spengler, T., Jiang, N., Campbell, M. S., Yandell, M. D., Manousaki, T., Meyer, A., Bloom, O. E., Morgan, J. R., Buxbaum, J. D., Sachidanandam, R., Sims, C., Garruss, A. S., Cook, M., Krumlauf, R., Wiedemann, L. M., Sower, S. A., Decatur, W. A., ... Li, W., 2013.

Sequencing of the sea lamprey (*Petromyzon marinus*) genome provides insights into vertebrate evolution. *Nat Genet.* 45(4), 415-21, 421e1-2.

Smith, V.J., Dyrzynda, E.A., 2015. Antimicrobial proteins: From old proteins, new tricks. *Mol. Immunol.* 68(2 Pt B), 383-98.

Smith, J. J., Timoshevskaya, N., Ye, C., Holt, C., Keinath, M. C., Parker, H. J., Cook, M. E., Hess, J. E., Narum, S. R., Lamanna, F., Kaessmann, H., Timoshevskiy, V. A., Waterbury, C., Saraceno, C., Wiedemann, L. M., Robb, S., Baker, C., Eichler, E. E., Hockman, D., Sauka-Spengler, T., ... Amemiya, C. T., 2018. The sea lamprey germline genome provides insights into programmed genome rearrangement and vertebrate evolution. *Nat Genet.* 50(2), 270-277. Erratum in: *Nat Genet.* 2018 50(11):1617.

Smolina, N., Khudiakov, A., Knyazeva, A., Zlotina, A., Sukhareva, K., Kondratov, K., Gogvadze, V., Zhivotovsky, B., Sejersen, T., Kostareva, A., 2020. Desmin mutations result in mitochondrial dysfunction regardless of their aggregation properties. *Biochim Biophys Acta Mol Basis Dis.* 1866(6), 165745.

Snyder, D.A., Rivers, A.M., Yokoe, H., Menco, B.P., Anholt, R.R., 1991. Olfactomedin: purification, characterization, and localization of a novel olfactory glycoprotein. *Biochemistry.* 30(38), 9143-53.

Speers-Roesch, B, Ip, Y.K., Ballantyne, J.S., 2006. Metabolic organization of freshwater, euryhaline, and marine elasmobranchs: implications for the evolution of energy metabolism in sharks and rays. *J Exp Biol.* 209(Pt 13), 2495-508.

Spiegel, R., Soiferman, D., Shaag, A., Shalev, S., Elpeleg, O., Saada, A., 2017. Novel Homozygous Missense Mutation in SPG20 Gene Results in Troyer Syndrome Associated with Mitochondrial Cytochrome c Oxidase Deficiency. *JIMD Rep.* 33, 55-60.

Stonell, L.M, Cake, M.H., Power, G.W., Potter, I.C. 1997. Comparisons Between the Kinetic Behaviour of the Muscle Carnitine Palmitoyltransferase I of a Higher and Lower Vertebrate. *Comparative Biochemistry and Physiology Part B: Biochemistry and Molecular Biology,* 118, 4, 845-850.

Sruthy, K.S., Nair, A., Antony, S.P., Puthumana, J., Singh, I.S.B., Philip, R., 2019. A histone H2A derived antimicrobial peptide, Fi-Histin from the Indian White shrimp, *Fenneropenaeus indicus*: Molecular and functional characterization. *Fish Shellfish Immunol.* 92, 667-679.

Tachibana, M., Kiyokawa, E., Hara, S., Iemura, S., Natsume, T., Manabe, T., Matsuda, M., 2009. Ankyrin repeat domain 28 (ANKRD28), a novel binding partner of DOCK180, promotes cell migration by regulating focal adhesion formation. *Exp Cell Res.* 315(5), 863-76.

Théry, C., Witwer, K.W., Aikawa, E., Alcaraz, M.J., Anderson, J.D., Andriantsitohaina, R., et al., 2018. Minimal information for studies of extracellular vesicles 2018 (MISEV2018): A position statement of the International Society for Extracellular Vesicles and update of the MISEV2014 guidelines. *J. Extracell. Vesicles.* 7, 1535750.

Tilwawala, R., Nguyen, S.H., Maurais, A.J., Nemmara, V.V., Nagar, M., Salinger, A.J., Nagpal, S., Weerapana, E., Thompson, P.R., 2018. The Rheumatoid Arthritis-Associated Citrullinome. *Cell. Chem. Biol.* 25, 691–704.e6

Torró-Montell, L., Cortés-Castell, E., Sirvent-Segura, E., Veciana-Galindo, C., Gil-Guillén, V., Rizo-Baeza, M., 2019. Influence of Olive Extracts on the Expression of Genes Involved in Lipid Metabolism in Medaka Fish. *Molecules*. 24(17), 3068.

Tsang, H.T., Edwards, T.L., Wang, X., Connell, J.W., Davies, R.J., Durrington, H.J., O'Kane, C.J., Luzio, J.P., Reid, E., 2009. The hereditary spastic paraplegia proteins NIPA1, spastin and spartin are inhibitors of mammalian BMP signalling. *Hum Mol Genet*. 18(20), 3805-21.

Turchinovich, A., Drapkina, O., Tonevitsky, A., 2019. Transcriptome of extracellular vesicles: State-of-the-art. *Front. Immunol*. 10, 202.

Uysal-Onganer, P., MacLatchy, A., Mahmoud, R., Kraev, I., Thompson, P.R., Inal, J., Lange, S., 2020. Peptidylarginine deiminase isozyme-specific PAD2, PAD3 and PAD4 inhibitors differentially modulate extracellular vesicle signatures and cell invasion in two glioblastoma multiforme cell lines. *Int. J. Mol. Sci*. 21 (4), pii E1495.

Vagner, T., Chin, A., Mariscal, J., Bannykh, S., Engman, D.M., Di Vizio, D., 2019. Protein composition reflects extracellular vesicle heterogeneity. *Proteomics*. 19 (8), e1800167.

van der Flier, L.G., Haegebarth, A., Stange, D.E., van de Wetering, M., Clevers, H., 2009. OLFM4 is a robust marker for stem cells in human intestine and marks a subset of colorectal cancer cells. *Gastroenterology*. 137(1), 15-7.

Villagra-Blanco, R., Silva, L.M.R., Conejeros, I., Taubert, A., Hermosilla, C., 2019. Pinniped- and Cetacean-Derived ETosis Contributes to Combating Emerging Apicomplexan Parasites (*Toxoplasma gondii*, *Neospora caninum*) Circulating in Marine Environments. *Biology (Basel)*. 8(1), 12.

Vincent, A., Berthel, E., Dacheux, E., Magnard, C., Venezia, N.L., 2016. BRCA1 affects protein phosphatase 6 signalling through its interaction with ANKRD28. *Biochem J*. 473(7), 949-60.

Vorobjeva, N.V., Chernyak, B.V., 2020. NETosis: Molecular Mechanisms, Role in Physiology and Pathology. *Biochemistry (Mosc)*. 85(10), 1178-1190.

Vossenaar, E.R., Zendman, A.J., van Venrooij, W.J., Pruijn, G.J., 2003. PAD, a growing family of citrullinating enzymes: genes, features and involvement in disease. *Bioessays*. 25 (11), 1106-18.

Wang, S., Wang, Y., 2013. Peptidylarginine deiminases in citrullination, gene regulation, health and pathogenesis. *Biochim. Biophys. Acta*. 1829 (10), 1126-35.

Wang, Y., Chen, Y., Guan, L., Zhang, H., Huang, Y., Johnson, C. H., Wu, Z., Gonzalez, F. J., Yu, A., Huang, P., Wang, Y., Yang, S., Chen, P., Fan, X., Huang, M., Bi, H., 2018a. Carnitine palmitoyltransferase 1C regulates cancer cell senescence through mitochondria-associated metabolic reprogramming. *Cell Death Differ*. 25(4), 735-748.

Wang, X.Y., Chen, S.H., Zhang, Y.N., Xu, C.F., 2018b. Olfactomedin-4 in digestive diseases: A mini-review. *World J Gastroenterol*. 24(17), 1881-1887.

Wang, X., Fei, F., Qu, J., Li, C., Li, Y., Zhang, S., 2018c. The role of septin 7 in physiology and pathological disease: A systematic review of current status. *J Cell Mol Med*. 22(7), 3298-3307.

Wang, H., Cheng, X., Li, M., Li, W., Zhu, T., Li, Q., 2019a. Adaptive immune stimuli altered the cargo proteins of exosomes released by supraneural myeloid body cells in *Lampetra japonica*. *Mol Immunol.* 111:64-72.

Wang, D., Gou, M., Hou, J., Pang, Y., Li, Q., 2019b. The role of serpin protein on the natural immune defense against pathogen infection in *Lampetra japonica*. *Fish Shellfish Immunol.* 92, 196-208.

Wang, C.C., Si, L.F., Li, W.Y., Zheng, J.L., 2019c. A functional gene encoding carnitine palmitoyltransferase 1 and its transcriptional and kinetic regulation during fasting in large yellow croaker. *Comp Biochem Physiol B Biochem Mol Biol.* 231, 26-33.

Wieser, T., 2004. Carnitine Palmitoyltransferase II Deficiency. [updated 2019 Jan 3]. In: Adam MP, Ardinger HH, Pagon RA, Wallace SE, Bean LH, Stephens K, Amemiya A, editors. *GeneReviews*® [Internet]. Seattle (WA): University of Washington, Seattle; 1993–2020. PMID: 20301431.

Wilkie, M.P., Turnbull, S., Bird, J., Wang, Y.S., Claude, J.F., Youson, J.H., 2004. Lamprey parasitism of sharks and teleosts: high capacity urea excretion in an extant vertebrate relic. *Comp Biochem Physiol A Mol Integr Physiol.* 138(4), 485-92.

Witalison, E.E., Thompson, P.R., Hofseth, L.J., 2015. Protein arginine deiminases and associated citrullination: physiological functions and diseases associated with dysregulation. *Curr. Drug Targets.* 16(7), 700-10.

Whitlock, J.M., Hartzell, H.C., 2017. Anoctamins/TMEM16 Proteins: Chloride Channels Flirting with Lipids and Extracellular Vesicles. *Annu Rev Physiol.* 79, 119-143.

Woo, S., Jeon, H.Y., Kim, S.R., Yum, S., 2011. Differentially displayed genes with oxygen depletion stress and transcriptional responses in the marine mussel, *Mytilus galloprovincialis*. *Comp Biochem Physiol Part D Genomics Proteomics.* 6(4), 348-56.

Wood, L.A., Brown, I.R., Youson, J.H., 1998. Characterization of the heat shock response in the gills of sea lampreys and a brook lamprey at different intervals of their life cycles. *Comp Biochem Physiol A Mol Integr Physiol.* 120(3), 509-18.

Wu, F., Feng, B., Ren, Y., Wu, D., Chen, Y., Huang, S., Chen, S., Xu, A., 2017. A pore-forming protein implements VLR-activated complement cytotoxicity in lamprey. *Cell Discov.* 3, 17033.

Xu, R., Greening, D.W., Rai, A., Ji, H., Simpson, R.J., 2015. Highly-purified exosomes and shed microvesicles isolated from the human colon cancer cell line LIM1863 by sequential centrifugal ultrafiltration are biochemically and functionally distinct. *Methods.* 87, 11-25.

Xu, Y., Zhu, S.W., Li, Q.W., 2016. Lamprey: a model for vertebrate evolutionary research. *Zool Res.* 37(5), 263-9.

Xu, R., Song, X., Su, P., Pang, Y., Li, Q., 2017. Identification and characterization of the lamprey Flotillin-1 gene with a role in cell adhesion. *Fish Shellfish Immunol.* 71, 286-294.

Xuan, Z.B., Wang, Y.J., Xie, J., 2019. ANO6 promotes cell proliferation and invasion in glioma through regulating the ERK signaling pathway. *Onco Targets Ther.* 12, 6721-6731.

Yang, H., Li, X., Ji, J., Yuan, C., Gao, X., Zhang, Y., Lu, C., Li, F., Zhang, X., 2019. Changes of microRNAs expression profiles from red swamp crayfish (*Procambarus clarkia*) hemolymph exosomes in response to WSSV infection. *Fish Shellfish Immunol.* 84, 169-177.

York, J.R., McCauley, D.W., 2020. Functional genetic analysis in a jawless vertebrate, the sea lamprey: insights into the developmental evolution of early vertebrates. *J Exp Biol.* 223(Pt Suppl 1), jeb206433.

Yu, Y., Huang, H., Wang, Y., Yu, Y., Yuan, S., Huang, S., Pan, M., Feng, K., Xu, A., 2008. A novel C1q family member of amphioxus was revealed to have a partial function of vertebrate C1q molecule. *J Immunol.* 181(10), 7024-32.

Zapata, M., Tanguy, A., David, E., Moraga, D., Riquelme, C., 2009. Transcriptomic response of *Argopecten purpuratus* post-larvae to copper exposure under experimental conditions. *Gene.* 442(1-2), 37-46.

Zhang, K., Tai, Z., Han, Q., Pang, Y., Li, Q., 2019. Adiponectin as inducer of inflammatory and apoptosis involving in immune defense in lamprey. *Fish Shellfish Immunol.* 90, 446-455.

Zhang, H., Li, S., Wang, F., Xiang, J., Li, F., 2020. Identification and functional study of an LRR domain containing membrane protein in *Litopenaeus vannamei*. *Dev Comp Immunol.* 109, 103713.

Zuo, Y., Yalavarthi, S., Shi, H., Gockman, K., Zuo, M., Madison, J.A., Blair, C., Weber, A., Barnes, B.J., Egeblad, M., Woods, R.J., Kanthi, Y., Knight, J.S. Neutrophil extracellular traps in COVID-19. *JCI Insight.* 2020 Jun 4;5(11), e138999.

## Figure legends

**Figure 1. EV characterisation of sea lamprey plasma-EVs by: A)** NTA analysis; **B)** Western blotting (WB) for the EV-specific markers CD63 and Flotillin-1 (the molecular size marker is indicated in kilo Daltons; kDa); **C)** Transmission electron microscopy (TEM) showing a poly-dispersed EV population and confirming EV morphology; scale bar indicates 50 nm.

**Figure 2. Lamprey deiminated protein and PAD identification. A.** A silver stained SDS-PAGE gel (4-20% gradient TGX gel), showing F95-enriched fractions from sea lamprey plasma and plasma-EVs, as indicated above each lane. The protein standard (std) is indicated in kilodaltons (kDa). **B.** The Venn diagram represents numbers of deiminated protein hits identified by LC-MS/MS from the F95 enriched fractions in plasma (plasma citrullinome) and plasma-EVs (EV citrullinome); uncharacterised protein hits are indicated in brackets. **C.** Western blotting analysis for PAD-like protein in sea lamprey plasma, using anti-human PAD1, PAD2, PAD3, PAD4 and PAD6 antibodies; strongest cross-reaction is observed with PAD2 and PAD6 antibodies; even amounts of samples were loaded on all gels for PAD-like protein detection. **D.** Detection of deiminated histone H3 (citH3) in lamprey plasma by western blotting observed at approximately 17 kDa. **E.** A neighbour joining tree shows reported lamprey PAD2-like protein sequences compared with teleost (sea bass *D. labrax*; rainbow trout *O. mykiss*) PAD-like proteins, amphibian (*X. laevis*) PAD-like protein, reptilian (*A. mississippiensis*) PAD1-3 isozymes and all five human (*H. sapiens*) PAD isozymes (PAD1, 2, 3, 4 and 6, respectively). The closest homology was found with human PAD2, followed by teleost (sea bass)

PAD. The red numbers represent a measure of support for the node. **F.** Percent identity matrix as generated by Clustal Omega for lamprey (*P. marinus*) PAD2-like protein sequences reported (XP\_0.382558.1; XP\_032825520.1; XP\_032825490.1), compared with human PADs 1-6 and sea bass (*D. labrax*) PAD (for the percent identity matrix including all sequences in the neighbour joining tree in E, see Supplementary Figure 1).

**Figure 3. Functional protein network analysis for deiminated proteins in lamprey plasma-EVs.** **A.** Protein-protein interaction networks are based on protein identifiers in human. PPI enrichment  $p$ -value:  $1.28 \times 10^{-11}$ . Colour coding for network interaction lines is included in the figure. **B.** Local network STRING analysis, pathways are shown by colour coding; **C-D.** KEGG pathways, pathways identified are highlighted by the colour coded nodes; **E-F.** Molecular function GO pathways are highlighted by colour coding of the nodes; **G-I.** Reactome pathways are indicated by the colour coded nodes.

**Figure 4. Functional protein network analysis for deiminated proteins identified in lamprey plasma.** **A.** The protein-protein interaction network is based on protein identifiers in human. PPI enrichment  $p$ -value:  $2.78 \times 10^{-15}$ . Colour coding for the network interaction lines is included in the figure. **B.** Local network STRING analysis, pathways are shown by colour coding; **C.** KEGG pathways, pathways identified are highlighted by the colour coded nodes; **D.** Molecular function GO pathways are highlighted by colour coding of the nodes; **E.** Reactome pathways are indicated by the colour coded nodes.

**Figure 5. Functional protein networks for deiminated proteins in lamprey plasma and plasma-EVs.** The number of common pathways, as well as plasma or plasma-EV specific pathways, is shown for STRING network cluster pathways, KEGG pathways, Molecular GO pathways and Reactome pathways.

### Supplementary Figures and Tables

**Supplementary Figure 1.** Percent identity matrix for sea lamprey PAD-like protein sequences compared with reported human, reptilian, amphibian and teleost PAD protein sequences (see neighbour joining tree in Figure 2E).

**Supplementary Figure 2.** **A.** SDS-PAGE silver stained gel (4-20% TGX gel) of lamprey plasma immunoprecipitated with the anti-human PAD2 antibody; the protein standard (Std) is indicated on the left in kilodaltons. **B.** Partial sequence alignment of the human PAD2 amino acid sequence with reported lamprey PAD2-like amino acid sequences to highlight the region of the human PAD2 (aa 100-200; see boxed regions) which was used as a peptide sequence to generate the anti-human PAD2 antibody (ab16478, Abcam). Sequence alignment was performed by clustal-omega; conserved sites between human and lamprey are highlighted by a star (\*).

**Supplementary Table 1.** F95 enriched proteins from sea lamprey plasma-EVs. Proteomic analysis, full LC-MS/MS results.

**Supplementary Table 2.** F95 enriched proteins from sea lamprey plasma. Proteomic analysis, full LC-MS/MS results.

**Figure 1:**

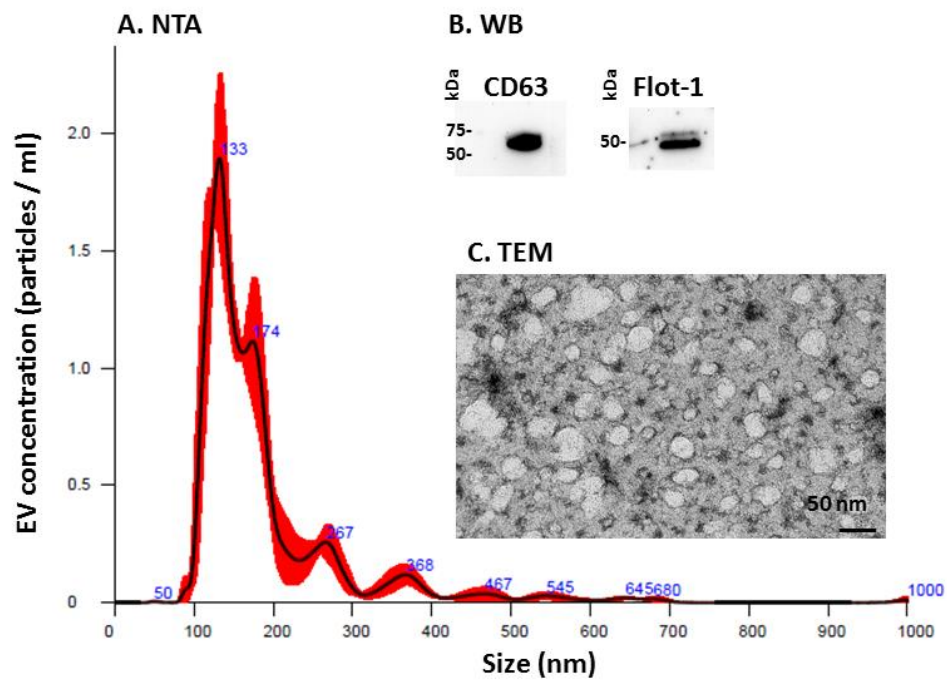
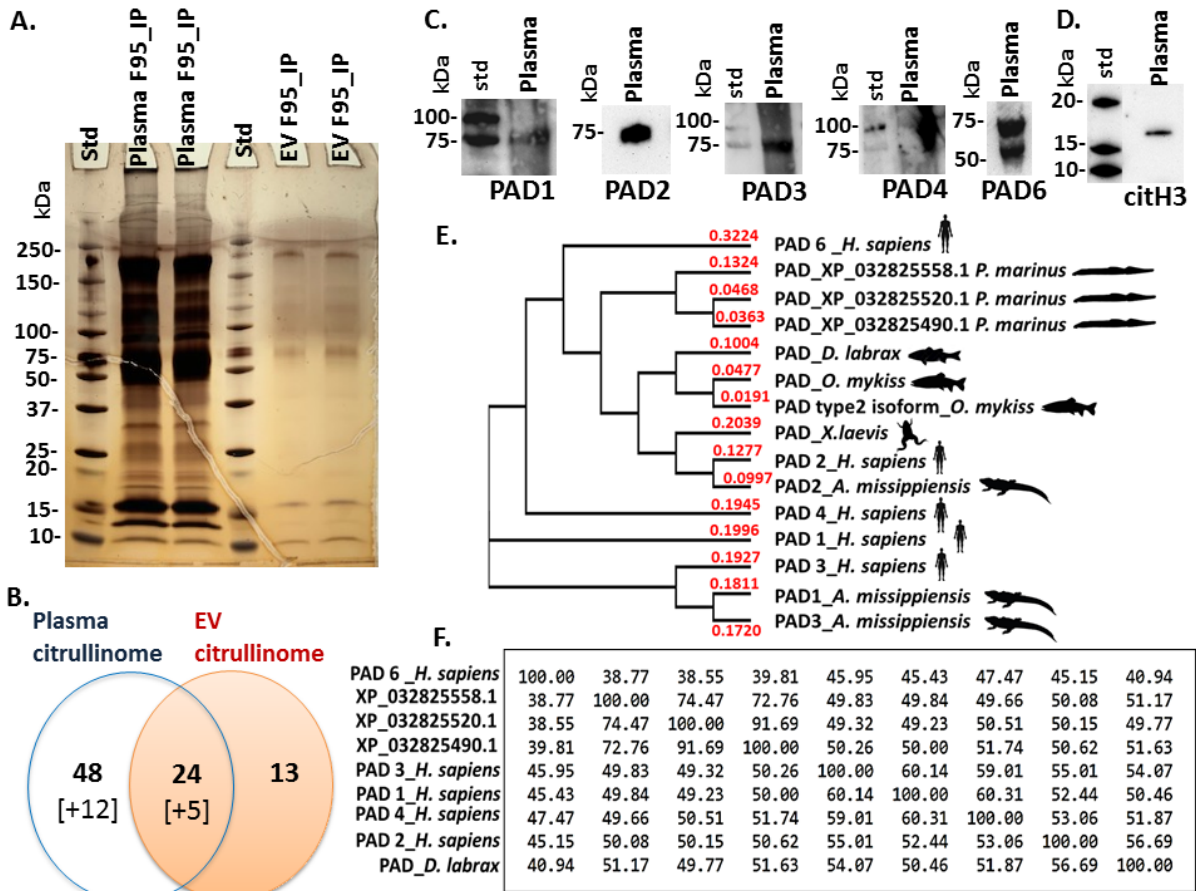


Figure 2:



Accepted Manuscript

Figure 3:

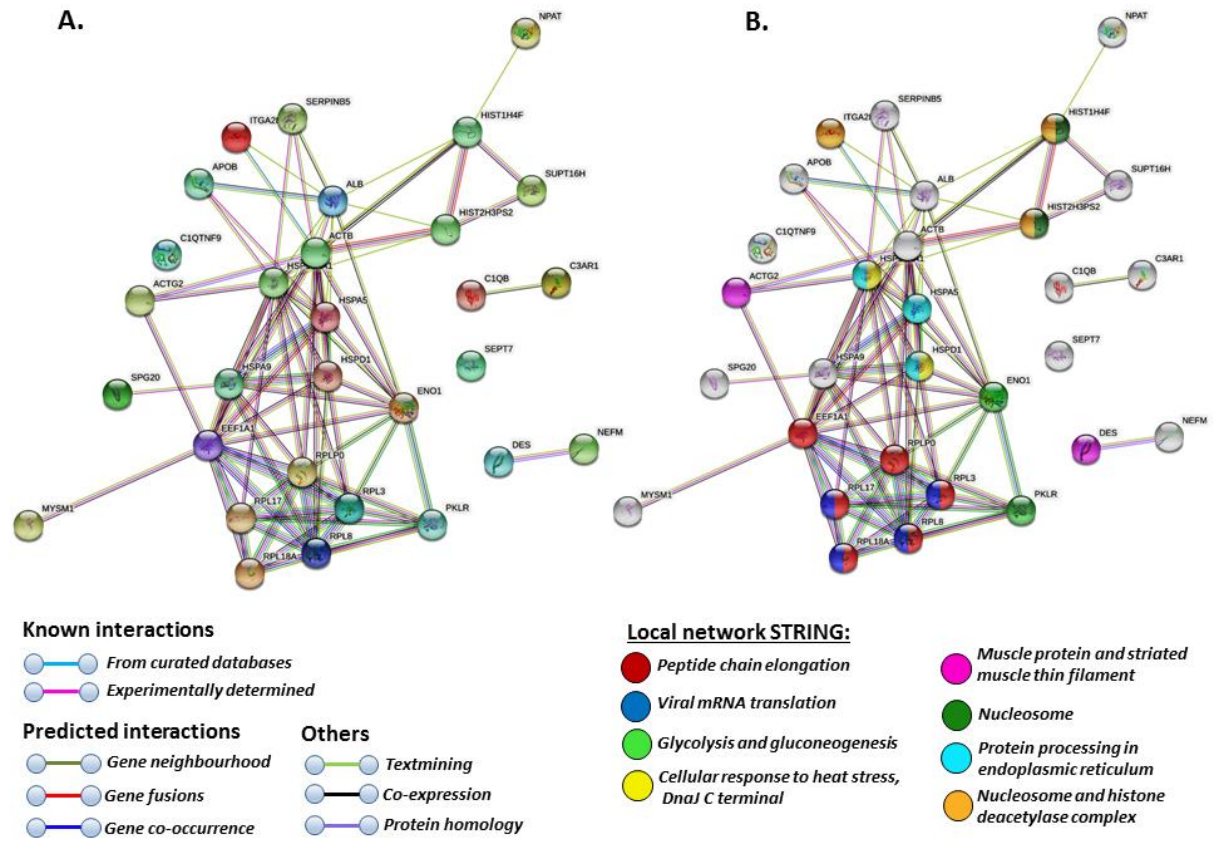


Fig 3A-B

Accepted Man

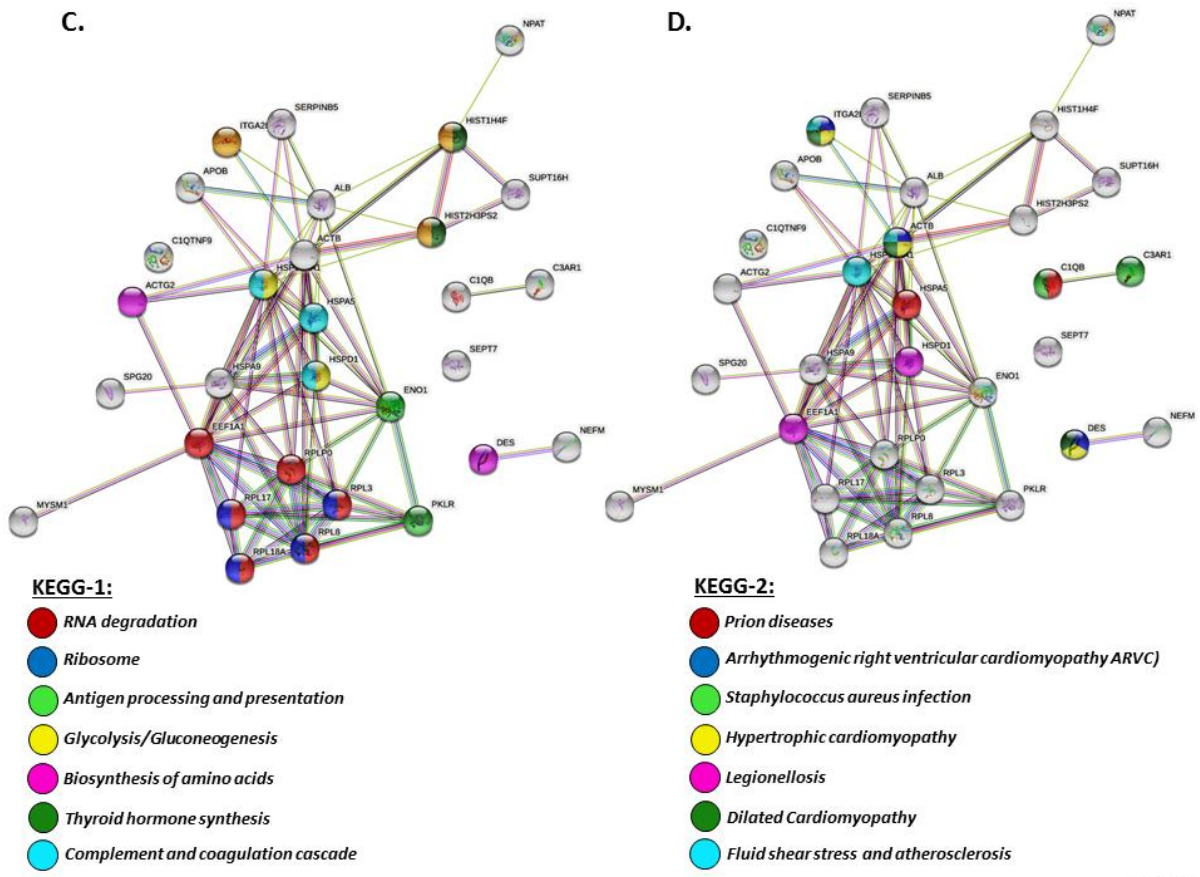


Fig 3C-D

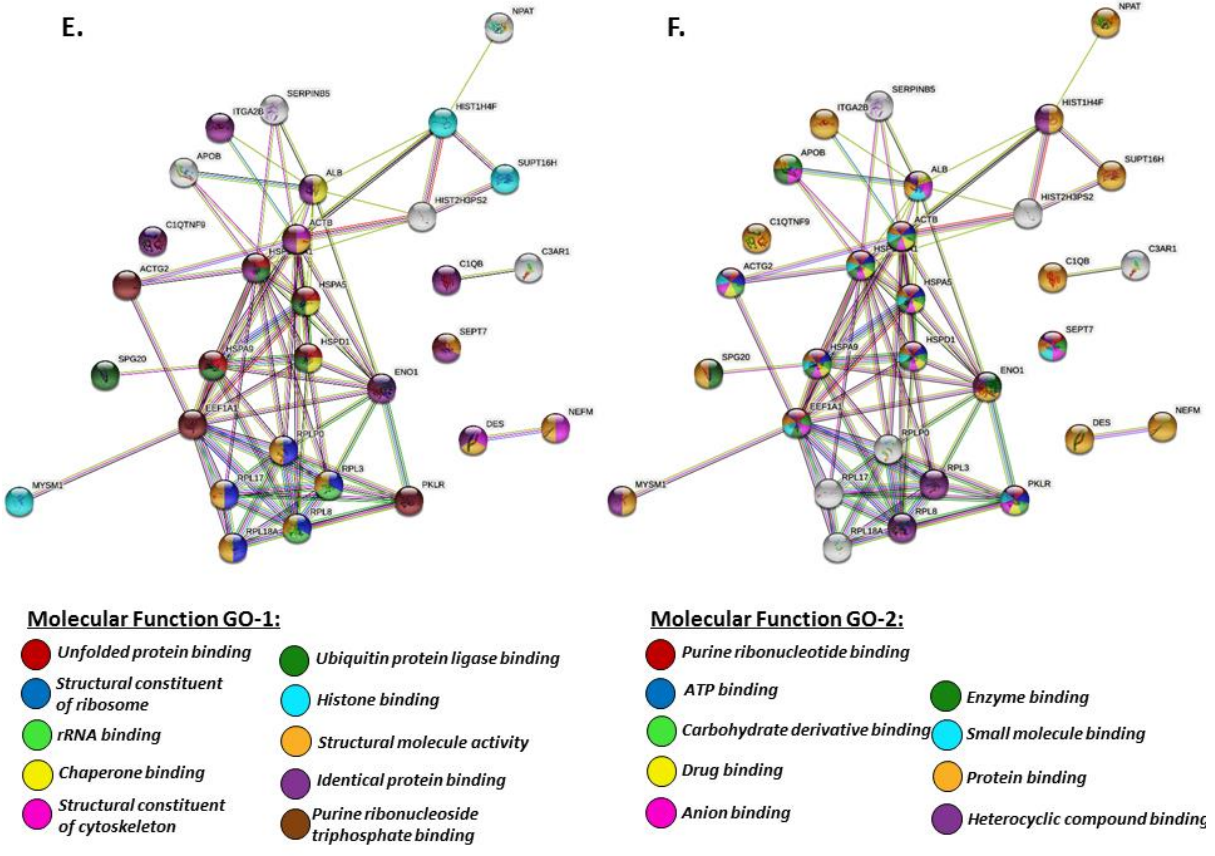
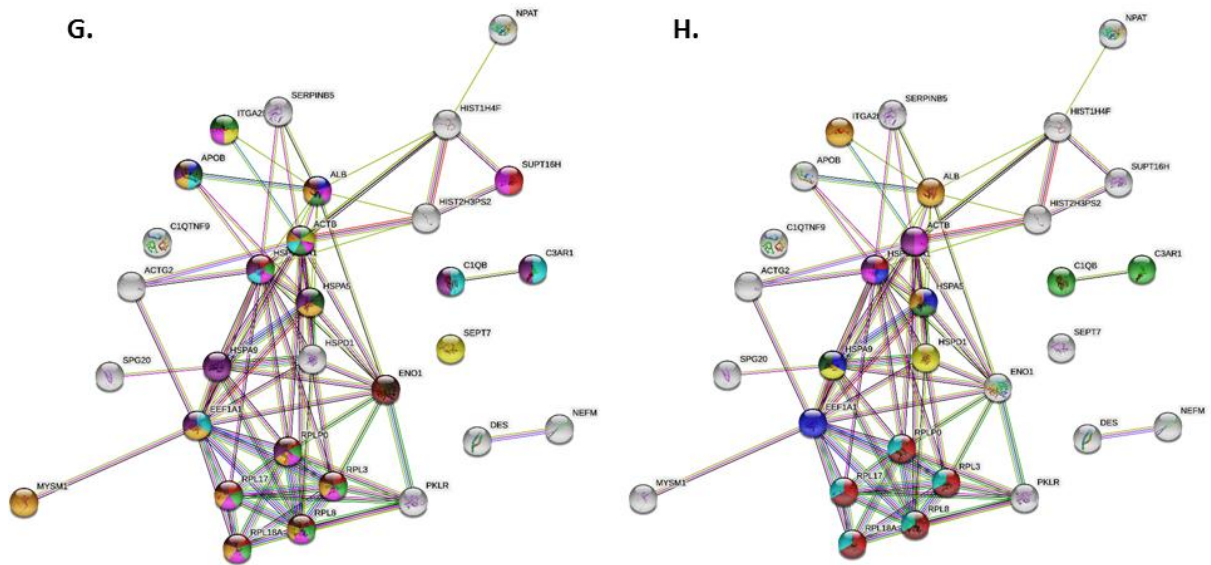


Fig 3E-F



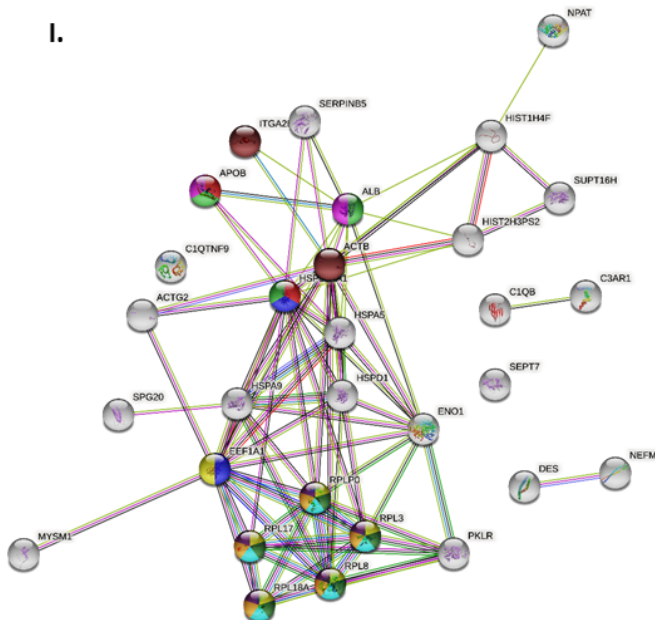
**Reactome-1:**

- Infectious disease
- Post-translational protein phosphorylation
- Axon guidance
- MAPK family signalling cascades
- Disease
- Haemostasis
- Innate immune system
- Metabolism of proteins
- Immune system
- Metabolism

**Reactome-2:**

- Influenza viral RNA transcription and replication
- Cellular response to heat stress
- Regulation of complement cascade
- Mitochondrial protein import
- Regulation of actin dynamics for phagocytic cup formation
- Regulation of HSF1-mediated heat shock response
- Major pathway of rRNA processing in the nucleus and cytoplasm
- Platelet degranulation
- VEGFA-VEGFR2 Pathway
- Nonsense mediated decay (NMD) enhanced by the exon junction

Fig 3G-H

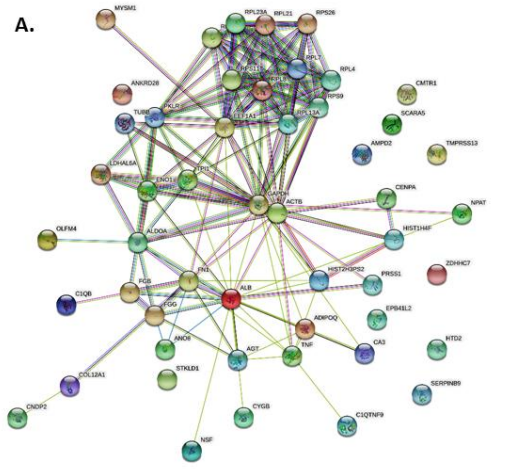


**Reactome-3:**

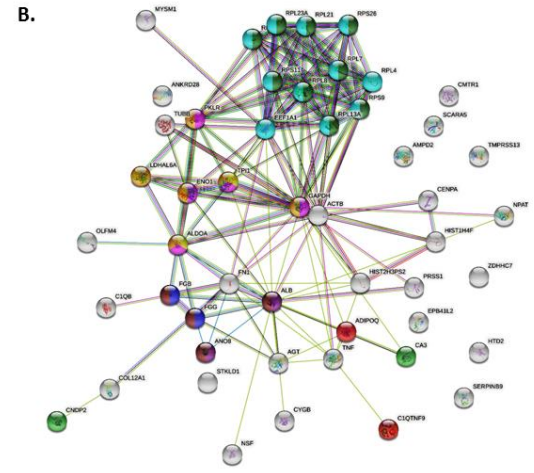
- Scavenging by class F receptors
- HSF1 activation
- Binding and uptake of ligands by scavenger receptors
- Peptide chain elongation
- Plasma lipoprotein remodelling
- Viral nRNA translation
- Eukaryotic translation termination
- Selenocysteine synthesis
- Nonsense mediated decay (NMD) independent of the exon
- MAPK2 and MAPK activation

Fig 3I

Figure 4:

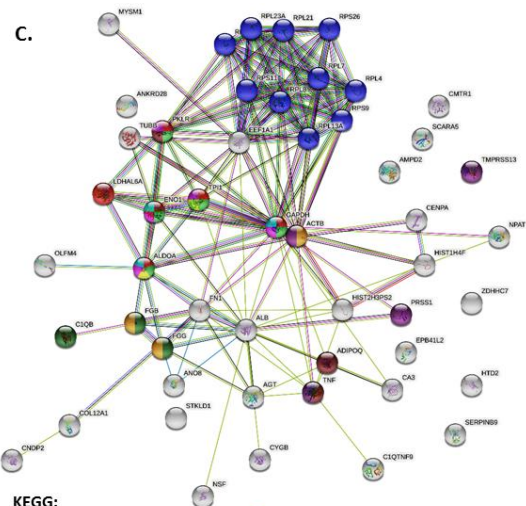


- Known interactions**
- From curated databases
  - Experimentally determined
- Predicted interactions**
- Gene neighbourhood
  - Gene fusions
  - Gene co-occurrence
- Others**
- Textmining
  - Co-expression
  - Protein homology

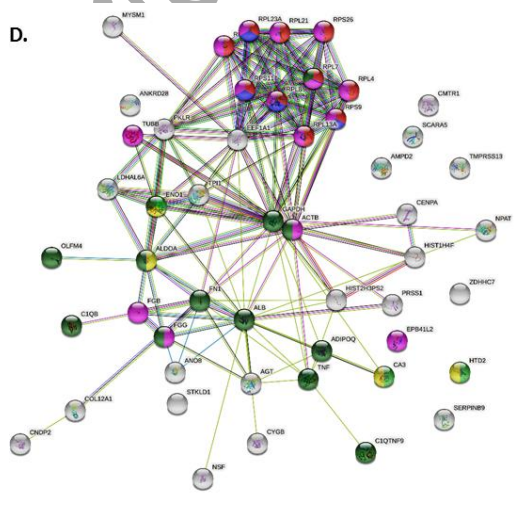


- Local network (STRING):**
- Adipokinetic hormone receptor activity
  - Fibrinogen alpha/beta chain family, peptidase 51A
  - Glutathione synthesis and recycling, arginine
  - Fructose 1,6-bisphosphate metabolic process
  - Glycolysis and gluconeogenesis
  - Viral mRNA translation
  - Peptide chain elongation
  - Carbon metabolism and lactate dehydrogenase activity
  - Post-translational protein phosphorylation
  - Regulation of insulin-like growth factor transport and clotting cascade

Fig 4A-B



- KEGG:**
- Glycolysis/gluconeogenesis
  - Ribosome
  - Biosynthesis of amino acids
  - Fructose and mannose metabolism
  - Carbon metabolism
  - Complement and coagulation cascades
  - HIF-1 signalling pathway
  - Platelet activation
  - Influenza A
  - Type II diabetes mellitus



- Molecular function GO:**
- Structural constituent of ribosome
  - rRNA binding
  - Hydro-lyase activity
  - Lyase activity
  - Structural molecule activity
  - Identical protein binding

Fig 4C-D

E.

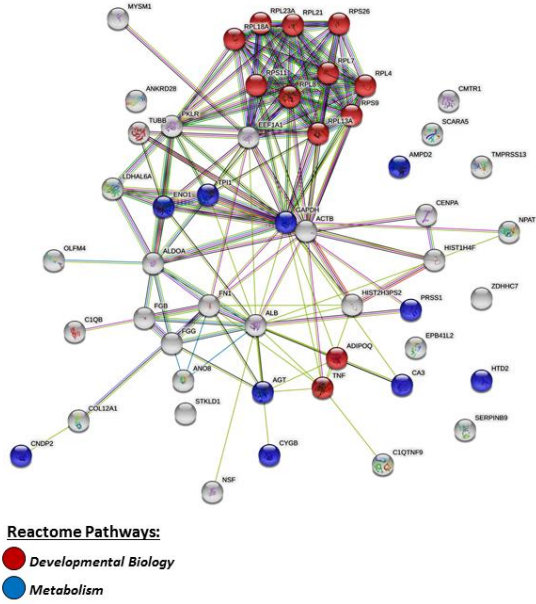


Fig 4E

Figure 5:

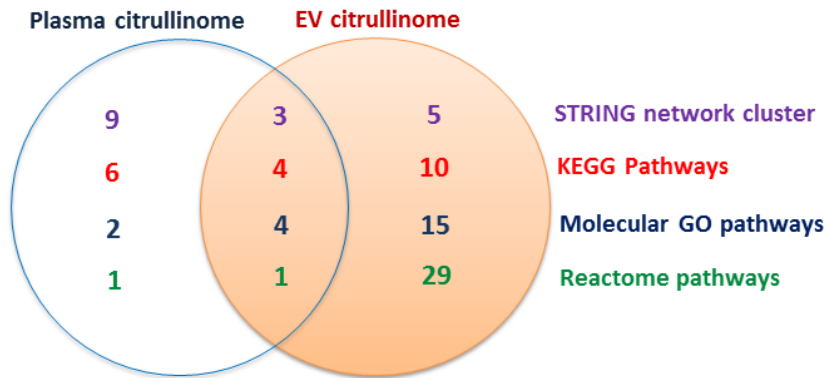


Fig 5

Accept

Supplementary Figure 1:

PAD 6_ <i>H. sapiens</i>	100.00	38.62	38.35	39.60	47.64	45.66	45.95	45.50	46.43	41.15	41.35	43.86	41.46	44.85
XP_032825558.1	38.62	100.00	74.47	72.76	50.00	49.61	50.00	48.60	51.01	51.09	51.56	55.23	48.04	49.92
XP_032825520.1	38.35	74.47	100.00	91.69	50.60	49.85	49.66	45.86	49.85	50.00	49.62	53.03	48.38	50.15
XP_032825490.1	39.60	72.76	91.69	100.00	52.00	50.47	50.52	48.37	51.09	51.86	51.56	55.03	48.83	50.46
PAD 4_ <i>H. sapiens</i>	47.64	50.00	50.60	52.00	100.00	60.48	59.01	59.01	61.97	52.04	51.71	52.05	50.60	53.40
PAD 1_ <i>H. sapiens</i>	45.66	49.61	49.85	50.47	60.48	100.00	60.03	61.48	58.73	50.31	49.69	53.69	50.46	52.82
PAD 3_ <i>H. sapiens</i>	45.95	50.00	49.66	50.52	59.01	60.03	100.00	61.12	62.71	54.24	53.91	54.10	52.49	55.16
PAD1_ <i>A. mississippiensis</i>	45.50	48.60	45.86	48.37	59.01	61.48	61.12	100.00	64.70	52.52	51.77	55.99	51.68	53.95
PAD3_ <i>A. mississippiensis</i>	46.43	51.01	49.85	51.09	61.97	58.73	62.71	64.70	100.00	52.13	53.37	55.90	52.91	56.75
PAD_ <i>D. labrax</i>	41.15	51.09	50.00	51.86	52.04	50.31	54.24	52.52	52.13	100.00	78.44	83.33	54.31	56.69
PAD_ <i>O. mykiss</i>	41.35	51.56	49.62	51.56	51.71	49.69	53.91	51.77	53.37	78.44	100.00	93.32	54.18	55.50
PAD type2 isoform_ <i>O. mykiss</i>	43.86	55.23	53.03	55.03	52.05	53.69	54.10	55.99	55.90	83.33	93.32	100.00	57.69	59.80
PAD_ <i>X. laevis</i>	41.46	48.04	48.38	48.83	50.60	50.46	52.49	51.68	52.91	54.31	54.18	57.69	100.00	61.04
PAD 2_ <i>H. sapiens</i>	44.85	49.92	50.15	50.46	53.40	52.82	55.16	53.95	56.75	56.69	55.50	59.80	61.04	100.00
PAD2_ <i>A. mississippiensis</i>	45.53	53.43	53.98	54.90	55.61	55.54	56.01	59.07	59.14	60.82	59.48	60.14	65.34	77.26

Supplementary Figure 2:

